

Cenozoic extension and magmatism in the North American Cordillera: the role of gravitational collapse

Mian Liu*

Department of Geological Sciences, University of Missouri, Columbia, MO 65211, USA

Abstract

Following a protracted phase (~ 155 – 60 Ma) of crustal shortening and mountain building, widespread extension and magmatism have dominated the tectonic history of the North American Cordillera since early Tertiary. Although decades of intensive investigations have made North American Cordillera one of the best studied continental regions in the world, many fundamental issues, including the cause of metamorphic core complexes and basin-and-range extension and their relationship with the overlapping magmatism, remain controversial. Recent studies have emphasized the role of gravitational collapse in causing both extension and magmatism in the Cordillera, but the geodynamics of gravitational collapse are not well understood. Using simple thermal–rheological and thermomechanical modeling, we address the following questions. (1) Could gravitational collapse of the thickened Cordilleran crust have formed the metamorphic core complexes? (2) Did gravitational collapse induce the intensive mid-Tertiary volcanism in the Cordillera? (3) What caused basin-and-range extension and the associated basaltic volcanism? Our results show that, although a thickened crust at isostatic equilibrium is dynamically unstable and tends to collapse, major postorogenic extension happens only when the lithosphere is sufficiently weakened by thermal processes associated with orogenesis, including thermal relaxation, radioactive heating, shear heating, and mantle thermal perturbations. Ductile spreading within the lower crust plays a major role in postorogenic gravitational collapse. This mechanism can explain most metamorphic core complexes and the associated plutonism. However, it is unlikely to have induced major mantle upwelling required by the voluminous silicic eruption during the mid-Tertiary. The cause of the mid-Tertiary mantle upwelling remains speculative, but strong mantle thermal perturbations under the northern Basin and Range province may have persisted since mid-Miocene. Thermomechanical modeling shows that this mantle upwelling may have caused significant ductile deformation within the surrounding lithosphere, with lithospheric material being pushed away and downward from the upwelling asthenosphere. The loci of maximum lithospheric thinning are near the margins of the upwelling mantle and have migrated outward during basin-and-range extension. This process can explain some of the spatial–temporal evolution of extension and volcanism in the Cordillera since mid-Miocene. The resultant lithospheric structures are consistent with geophysical observations in the Basin and Range province. © 2001 Elsevier Science B.V. All rights reserved.

Keywords: Extension; Magmatism; North American Cordillera; Basin and Range; Metamorphic core complex

1. Introduction

From crustal shortening to postorogenic extension, magmatism occurs in all phases of orogenesis. However, the cause of these magmas and their geodynam-

* Tel.: +1-573-882-3784; fax: +1-573-882-5458.
E-mail address: lium@missouri.edu (M. Liu).

ical relationship to crustal deformation are often controversial. This is well illustrated by the Cenozoic extension and magmatism in the North American Cordillera (Fig. 1), where major crustal extension started a few to tens of million years after the Cordilleran orogeny (~ 155 –60 Ma) and overlapped with widespread magmatism in space and time (Fig. 2). After decades of studies, the relationship between the Cordilleran extension and magmatism remains a topic of hot debate (see a collection of recent papers in numerous special volumes in the *Journal of Geophysical Research* (June 1989, July 1991, June 1995) and other publications (Coward et al., 1987; Mayer, 1986)).

One of the major issues under debate is the formation of metamorphic core complexes and their dynamic interplay with the overlapping magmatism (Armstrong, 1982; Coney, 1980; Coney and Harms, 1984; Liu and Shen, 1998a; Livaccari, 1991; Sonder et al., 1987; Vanderhaeghe and Teyssier, 1997; Wernicke et al., 1987; Zoback et al., 1981). In many places of the Cordillera, the inception of major crustal

extension was marked by the development of metamorphic core complexes, the high-grade metamorphic rocks of the middle crust exposed by crustal extension along gentle-dipping shear zones (Armstrong, 1982; Coney, 1980). Occurrence of many core complexes along the core zone of thickened crust in the Cordilleran orogen (see Fig. 2) indicates a cause of gravitational collapse (Coney and Harms, 1984). However, given the relatively uniform crustal contraction during the Cordillera orogeny (Elison, 1991), the instability of overthickened crust alone cannot readily explain the diachronous development of the core complexes. North of the Snake River Plain, extension began mainly in early Eocene. Farther south, the inception time was largely Oligocene in the Great Basin, and slightly later in the Mojave–Sonora desert region. Extension in areas near the latitude of Las Vegas did not occur until mid-Miocene (Wernicke et al., 1987). Wernicke et al. (1987) noticed the close correlation between the onset time of crustal extension and the abundance of coeval plutons, but the cause of the plutons is not clear.

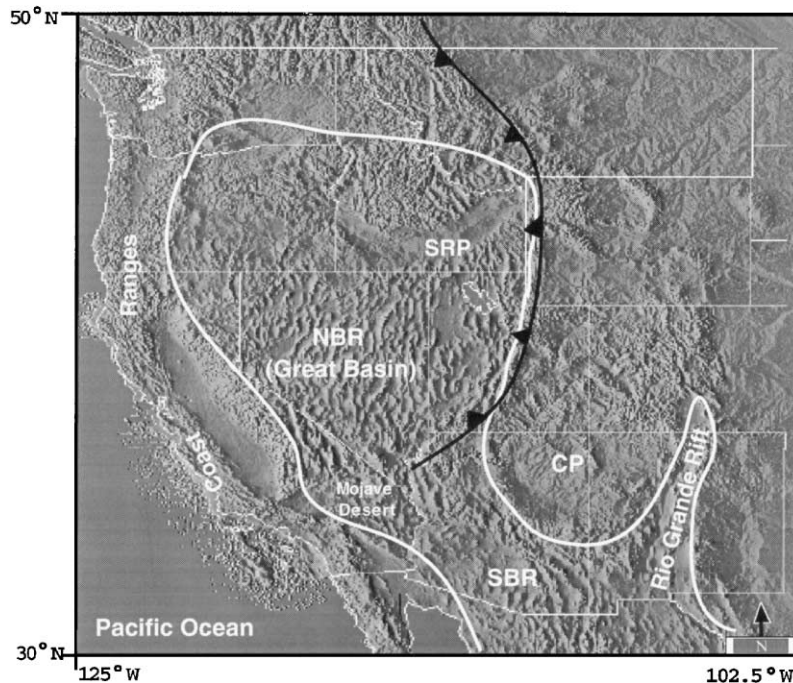


Fig. 1. Topographic relief map of the North American Cordillera. The tooth curve shows the eastern boundary of the Cordilleran fold-and-thrust belts. The solid white line indicates the boundary of the Basin and Range province. Abbreviations are as follows: NBR, northern Basin and Range, also called the Great Basin; SRB, southern Basin and Range; SRP, Snake River Plain; and CP, Colorado Plateau.

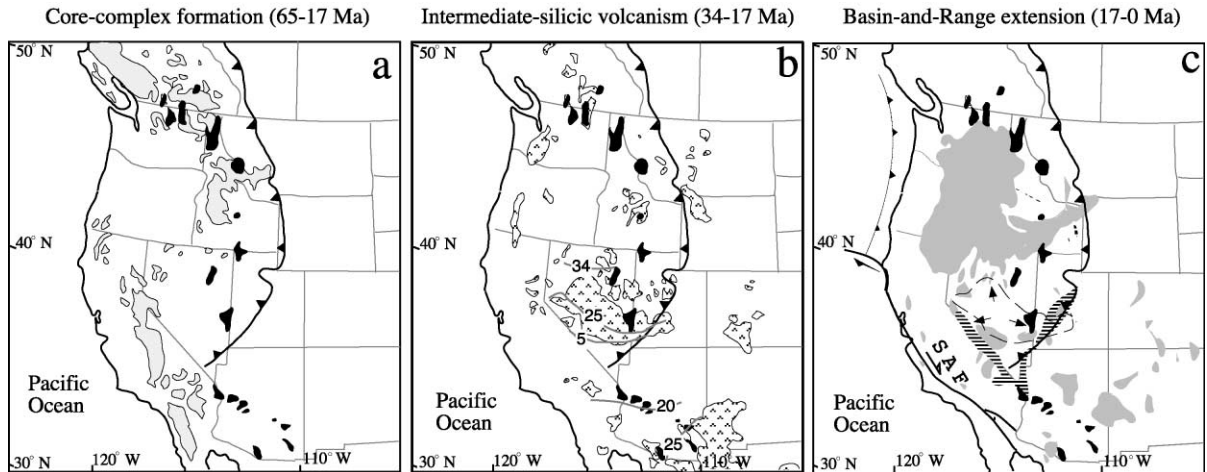


Fig. 2. Simplified maps showing major development of Cenozoic extension and magmatism in the Cordillera. (a) Distribution of late Mesozoic to Cenozoic granitic batholiths (shaded areas) and Tertiary metamorphic core complexes (dark areas) in the North American Cordillera. The tooth curve indicates the eastern boundary of the Cordilleran fold-and-thrust belts. (b) Early to Middle Tertiary intermediate-silicic rocks (patterned areas). Gray lines with numbers (in Ma) are isochrons of intermediate-silicic magmatic front. (c) Basalt and bimodal volcanism (gray areas) and major extension (areas of horizontal bars) since mid-Miocene. Short arrows indicate the direction of migration of extension and volcanism. SAF: the San Andreas Fault. After Stewart (1978) and Wernicke et al. (1987).

Another problem of the Cordilleran tectonics is the eruption of voluminous intermediate-silicic material in the Great Basin (the northern Basin and Range province) and its apparent lack of spatial or temporal correlation with crustal extension (Fig. 2b). During mid-Tertiary, magmatism swept southward across the Great Basin in generally E–W trending belts. The magmatism culminated between 34 and 17 Ma when more than $50,000 \text{ km}^3$ volcanic ash erupted over an area of $> 71,000 \text{ km}^2$ (Best and Christiansen, 1991). Considering the massive intrusive rocks as indicated by exposed large-volume subvolcanic magma chambers, the total volume of magma is likely much greater (Lipman and Glazner, 1991). Although in many regions, magmatism and extension closely overlapped over time and space (Gans et al., 1989), some recent studies suggest that the temporal–spatial correlation was poor on a provincial scale (Axen et al., 1993; Best and Christiansen, 1991; Taylor et al., 1989). The peak volcanism in central Great Basin between 34 and 17 Ma was accompanied by limited extension (Best and Christiansen, 1991). Most basin-and-range extension occurred $\sim 10 \text{ m.y.}$ after the peak silicic volcanism and was concentrated near the margins of the main volcanic field in central Great Basin (Fig. 2c). This spatial–temporal pattern of extension and magmatism does not

fit the simple “active” or “passive” rifting models of Sengor and Burke (1978). Some studies attributed the volcanism to foundering of the subducting Farallon slab (Lipman et al., 1971, 1972), others explained the volcanism as the consequence of gravitational collapse of the Cordillera orogen (Harry and Leeman, 1995; Leeman and Harry, 1993; Wernicke et al., 1987).

The cause of basin-and-range extension and the associated basaltic volcanism is also an issue of considerable controversy (Coney, 1987; Wernicke, 1992; Zoback et al., 1981). Since mid-Miocene, large volume of flood basalts erupted over the Columbia plateau, whereas in other places, intermediate-silicic magmatism was followed by basaltic–rhyolitic bimodal and eventually basaltic volcanism (Fig. 2c). However, only in the Basin and Range province and the Rio Grande Rift was basaltic magmatism associated with major extension in time and space. This young phase of extension, which was chiefly responsible for the present basin–range physiography, was characterized by deep (10–15 km) penetrating block faults, in contrast to the low-angle detachment faults associated with core-complex formation. Geodetic measurements show that the Great Basin is presently extending with strain rates between $3 \times 10^{-16} \text{ s}^{-1}$ and $5 \times 10^{-16} \text{ s}^{-1}$ (Bennette et al., 1998; Dixon et al., 1995). Some

workers suggested that the basin-and-range faults are the near-surface counterpart of the deeper low-angle detachment faults, which are now exposed in metamorphic core complexes (e.g., Gans et al., 1989). Others believed that the different faulting styles, tectonic environments, and associated volcanism between these two types of extensional faults are indicative of fundamentally different origins (see review by Burchfiel et al., 1992 and references therein).

Resolving these issues requires a better understanding of the underlying driving forces for the extension and magmatism in the Cordillera. The proposed driving forces for the Cordilleran extension fall into three categories (Liu, 1996; Sonder and Jones, 1999; Wernicke, 1992): (1) far-field forces originated at plate boundaries, (2) forces acting on the base of the lithosphere due to upwelling mantle, and (3) buoyancy forces arising from within the orogenic lithosphere because of lateral density variations. Following Atwater (1970), many workers relate Cordilleran tectonics to interactions between the North America plate and the oceanic Farallon and Pacific plates. Since ~ 29 Ma, the convergent plate boundary (subduction of the Farallon plate under North America) has been gradually replaced by the transform boundary along the San Andreas Fault system. This may have caused relaxation of compressional stresses and facilitated the Cordilleran extension, as indicated by $\sim 45^\circ$ change of least principle stress orientation in the Great Basin over the past 10 m.y. (Zoback et al., 1981). However, plate boundary forces alone cannot fully explain Cenozoic extension in the Cordillera, especially early Tertiary extension in many places when the plate boundary along western North America was compressional and crustal extension was coeval to compressional tectonics to its west (Wernicke et al., 1987). Mantle thermal perturbations were clearly associated with Cordilleran extension and volcanism, but their cause and relationship to extension remain speculative (Bird, 1979; Dickinson and Snyder, 1979; Lipman, 1980; Parsons et al., 1994; Saltus and Lachenbruch, 1991). Enlightened by active extension in mountain belts at convergent plate boundaries, increasing number of studies in recent years have emphasized the role of gravitational collapse (Coney and Harms, 1984; Dilek and Moores, 1999; Harry et al., 1993; Jones et al., 1996; Livaccari, 1991; Sonder et al., 1987; Sonder and Jones, 1999; Wernicke et al., 1987).

Despite the wide acceptance of gravitational collapse as a viable explanation for extension in orogens, this mechanism is not well understood. For instance, some studies suggest that gravitational collapse of the thickened orogenic crust can cause significant whole-lithosphere extension (Govers and Wortel, 1993; Harry et al., 1993), other models show that gravitational collapse of the crustal welt may be largely decoupled from the mantle lithosphere (Bird, 1991; Liu and Shen, 1998a). Most workers recognize that perhaps no single cause or driving force can explain all extensional tectonics in the Cordillera (Coney, 1987; Liu and Shen, 1998a; Sonder and Jones, 1999; Zoback et al., 1981). This paper explores the role and limitations of gravitational collapse in the Cordilleran tectonics. We focus on gravitational collapse because it can be better constrained relative to plate boundary and mantle processes. Isolating the effects of gravitational collapse would help us to better understand the roles of other driving forces. In the following, we first discuss the geodynamics of gravitational collapse of orogens. We then apply the geodynamic constraints to Cenozoic extension and magmatism in the Cordillera. We do not intend to present a complete geodynamic model of the Cordilleran extension and volcanism, which is beyond the scope of this study. Rather, we use simple thermal–rheological and thermomechanical models to illustrate some of the basic physics of gravitational collapse that will help to address these questions: (1) Could gravitational collapse of the thickened Cordilleran crust have formed metamorphic core complexes? How did core-complex formation relate to the associated plutonism? (2) Was gravitational collapse the major cause of the voluminous mid-Tertiary volcanism? (3) How was basin-and-range extension related to the core-complex formation?

2. Geodynamics of gravitational collapse

Gravitational collapse of orogens is driven by excess gravitational potential energy in the orogens when the elevated topography is supported by buoyancy forces within the lithosphere (Artyushkov, 1973; Molnar and Lyon-Caen, 1988). In most cases, the buoyancy forces arise from crustal thickening or mantle thermal perturbations (England, 1993; Molnar

and Lyon-Caen, 1988). Although extension in many orogens involved both crustal thickening and mantle upwelling, the effects of these two factors and their dynamic relationship are often ambiguous (Liu and Shen, 1998a). To isolate the controlling parameters of gravitational collapse and to understand the dynamic interplay between crustal thickening and mantle upwelling, we discuss these two processes separately.

2.1. Gravitational collapse of a thickened crust

The principles of gravitational collapse are often illustrated by the dynamic instability of a thickened crust at isostatic equilibrium (Artyushkov, 1973; Molnar and Lyon-Caen, 1988; Sonder et al., 1987) (Fig. 3). The formation of many core complexes in the zone of thickest Cordilleran crust is a major piece of evidence for gravitational collapse in the Cordillera (Coney and Harms, 1984). The mechanics of gravitational collapse of a thickened crust and the dynamic consequences, however, have not been fully understood. In this section, we discuss the stress states, thermal–rheological evolution, and magmatism associated with extension of thickened orogenic crust.

2.1.1. Stress state and synorogenic extension

It has been shown that orogenic belts with a thickened crust may be unstable and tends to collapse

under its own weight (Artyushkov, 1973; Bott and Dean, 1972; Fleitout and Froidevaux, 1982; Le Pichon, 1982; Molnar and Lyon-Caen, 1988). The buoyancy force (per unit length) driving extension arises from the differential pressure between two lithospheric columns:

$$F = \int_{-h}^l \Delta P(z) dz, \tag{1}$$

where $\Delta P(z) = \int_{-h}^z \Delta \rho(z) g z dz$ is the pressure difference at depth z , $\Delta \rho$ is the density difference at depth z , g is the gravitational acceleration, h is the elevation of the mountain range above the reference lowland, and l is the compensation depth. For a crustal welt at a simple Airy-type isostasy (Fig. 3), Eq. (1) can be written as

$$F = \int_{-h}^l \Delta \rho g z dz, \tag{2}$$

thus, the buoyancy force takes the form of differences in gravitational potential energy per unit area (Molnar and Lyon-Caen, 1988), and l can be defined at the base of the thickened crust. As shown in Fig. 3, isostasy implies only a vertical force balance. At any given depth above l , the lithostatic pressure under the thickened crust is greater than that under the surrounding lowland. This lateral pressure difference

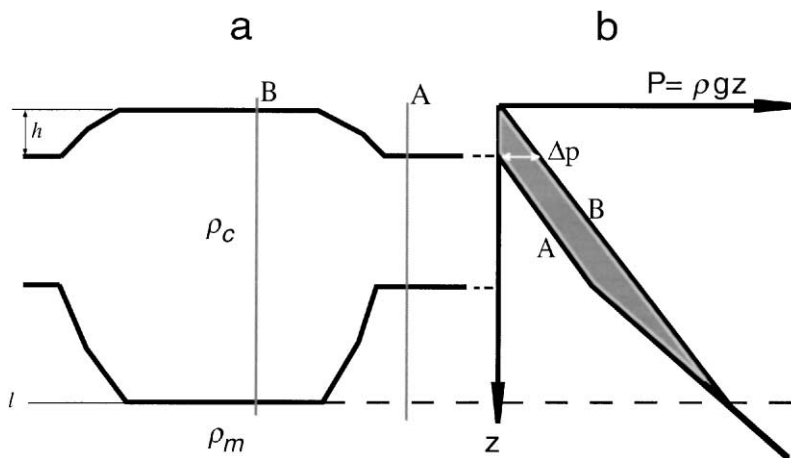


Fig. 3. Conceptual model of gravitational collapse of a thickened crust. (a) Sketch of a thickened crust at Airy-type isostasy. (b) Lithostatic pressures along vertical profiles across the lowland crust (line A) and the mountain range (line B). The differential pressure Δp tends to cause crustal collapse.

tends to collapse the crustal welt. Assuming constant crustal and mantle density and a complete Airy isostasy, F can be estimated from crustal thickness and elevation (Liu and Shen, 1998a; Molnar and Lyon-Caen, 1988):

$$F = \rho_c g h \left(H_r + \frac{h + \Delta H}{2} \right), \quad (3)$$

where ρ_c is crustal density, H_t and H_r are the thickness of the thickened and reference crust, respectively, and $h = (\rho_m - \rho_c)(H_t - H_r)/\rho_m$ is the isostatically supported elevation, where ρ_m is the mantle density. For major orogenic belts where the crustal thickness is > 60 km, the buoyancy force per unit length is on the order of 10^{12} N/m, comparable with typical tectonic forces associated with ridge push and slab pull (Bott, 1993; Forsyth and Uyeda, 1975).

During orogenesis, the buoyancy force within the lithosphere is counter-balanced by tectonic compressional forces.

The synorogenic stress state within orogenic crust has been investigated in numerous studies (Artyushkov, 1973; Liu et al., 2000; Smrekar and Solomon, 1992). In Fig. 4, we show the deviatoric stresses within a crustal welt calculated using a viscoelastic finite element code (Liu et al., 2000). A 5-km elevation of the crustal welt is isostatically compensated by an Airy-type crustal root. The top 20 km of the crust is elastic, the rest of the crust assumes a power-law flow rheology of granite (Kirby and Kronenberg, 1987). Model parameters and rheological values are given in Tables 1 and 2, respectively. The top is a free surface, and the Winkler spring foundation is used on the bottom to simulate the effects of isostatic restoring force (Williams and Richardson, 1991). The left side is a symmetric boundary; the right side is a no-displacement boundary, equivalent to applying an average ~ 70 MPa compressional stress in this case. The stresses in Fig. 4 are nonlithostatic stresses due to the topographic

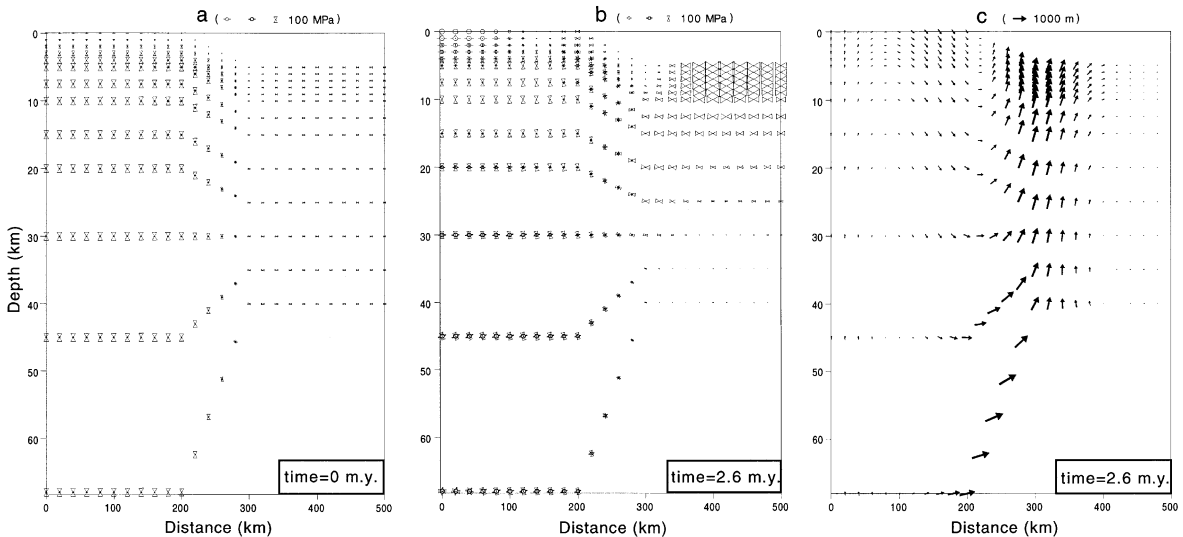


Fig. 4. (a) Initial non-lithostatic stresses within a crustal welt isostatically supported by an Airy-type crustal root. The bow-ties are the principal stresses of maximum compression (σ_1), the circles with short bars are the principal stresses of minimum compression (σ_2) with positive values (compressional), and the dotted circles with short bars are σ_2 with negative values (tensile). Scales of stresses are shown in the parenthesis. The top 20 km is elastic media, and the rest is ductile crust with a power-law flow rheology (see text). The left side is a symmetric boundary; the right side is fixed. The top is a free surface, and Winkler spring foundation is used on the bottom to simulate the effects of isostatic restoring forces. (b) Non-lithostatic stresses after 2.6 Ma when shear stresses ($|\sigma_1 - \sigma_2|$) in the ductile crust are largely erased by viscous relaxation, as indicated by nearly equal magnitudes of σ_1 and σ_2 in the lower crust. The stress states within the top 15 km of the crustal welt are extensional, as indicated by the nearly vertical σ_1 and small to negative (tensile) σ_2 . (c) Accumulative displacement field showing gravitational spreading of the overthickened crustal welt. See text for further discussion.

Table 1
Model parameters

Parameter	Definition	Value
A_0	volumetric radioactive heating (surface value)	$2 \mu\text{W}/\text{m}^3$
C_p	specific heat	1000 J/kg K
d	characteristic length scale of radioactive heating	10 km
κ	thermal diffusivity	$10^{-6} \text{ m}^2/\text{s}$
L	latent heat of fusion	420 kJ/kg
ρ_c	density of crust	2800 kg/m ³
ρ_m	density of the mantle	3300 kg/m ³
ρ_a	density of the asthenosphere	3200 kg/m ³
μ	frictional coefficient	0.65

loading and lateral tectonic compression. Fig. 4a shows the elastic solution of stresses. The maximum compressional stresses (σ_1) is vertical under the plateau and reaches its maximum value at the base of the plateau. Below that, the stresses do not increase with depth because the lithostatic stresses are removed. The stress state in Fig. 4a, however, is not common in orogens because it can be quickly changed by viscous relaxation within the ductile crust (Fig. 4b). The rate of viscous relaxation is indicated by the Maxwell relaxation time τ_m , essentially the ratio of the effective viscosity to the shear modulus of a viscoelastic body. It is the time needed for the deviatoric stresses to drop by a factor of $1/e$ by viscous relaxation (Ranalli, 1995). For the lower crust under orogens, the Maxwell time is generally less than 0.1 m.y. for dried diabase and $<10^{-3}$ m.y. for granitic material (Shen, 1997). Fig. 4b shows the stress state after 2.6 m.y. when the shear stresses have largely vanished within the ductile crust, indicated by the near equal magnitudes of σ_1 and σ_2 . Note the stress amplification within the upper crust (compare with Fig. 4a). The stresses are extensional under the crustal welt, indicated by the vertical σ_1 and small to negative (tensile) σ_2 . The maximum compression is found near the foothills within the lowland. Including the Coulomb–Navier failure criterion in the model, Liu et al. (2000) showed that significant crustal extension may occur in the plateau, with coeval thrusting near the foothills. The faulting pattern is comparable with deformation in active orogenic belts including the Tibetan plateau and the Andes (Armijo et al., 1986; Mercier, 1981; Mercier et al., 1992). The accumulated

displacement field (Fig. 4c) shows gravitational spreading of the crustal welt. Liu et al. (2000) showed that the major parameters controlling the stress state and crustal deformation include the elevation of orogens, the rheological structure of the crust, the magnitude of tectonic compression, and the three-dimensional boundary conditions. In general, synorogenic extensional faulting is restricted to the upper crust, and the faulting patterns are controlled by regional tectonic compression and topographic variations of orogens. Limited synorogenic extension may have occurred in the Cordillera, but overprinting by later tectonic events has made their recognition difficult (Hodges and Walker, 1992).

2.1.2. Thermal–rheological evolution and postorogenic crustal collapse

The geodynamic link between the synorogenic extension and the widespread postorogenic extension in the Cordillera remains uncertain. Clearly, the synorogenic extension did not lead directly to postorogenic extension in most regions, as most postorogenic extension in the Cordillera occurred tens of million years after the orogeny (Glazner and Bartley, 1985; Wernicke et al., 1987). Similar time gap between the end of orogeny and major postorogenic extension is found in many other orogens (Dewey, 1988; Glazner and Bartley, 1985). Lynch and Morgan (1987) suggested that major extension may require the extensional force to overcome the mechanical strength of the lithosphere. Thus, this time gap may indicate the time needed for postorogenic thermal processes to sufficiently weaken the lithosphere (Glazner and Bartley, 1985).

Thermal evolution related to orogenesis has been studied intensively (England and Richardson, 1977; England and Thompson, 1984; Liu and Furlong,

Table 2
Flow law parameters

	A	H (kJ/mol)	n	References
Granite	$10^{-8.8}$	123	3	Kirby and Kronenberg (1987)
Diabase	$10^{-3.7}$	260	3.4	Kirby and Kronenberg (1987)
Olivine	$10^{3.28}$	420	3	Rutter and Brodie (1988)

1993; Oxburgh and Turcotte, 1974; Peacock, 1989; Ruppel et al., 1988; Shi and Wang, 1987). Transient thermal structure of the lithosphere associated with crustal thickening and extension is governed by the heat equation:

$$\frac{\partial T}{\partial t} = \kappa \nabla^2 T - \vec{u} \cdot \nabla T + Q, \quad (4)$$

where T is the temperature, \vec{u} is the velocity vector for advection and erosion, κ is thermal diffusivity, C_p is the specific heat, and Q is the heat source (or sink) associated with radioactive heating, friction (or shear) heating, and latent heat due to fusion (Liu and Chase, 1991) (Table 1).

During synorogenic crustal thickening, the thermal structure of the lithosphere is controlled by both conduction and advection related to thrusting of crustal sheets. The relative importance of these two processes is indicated by the Peclet number Pe , which is essentially the ratio of heat transferred by advection to that by conduction and is defined as $Pe = vl/\kappa$, where v is the velocity of heat emplacement by the thrusting sheets and l is the characteristic length. Oxburgh and Turcotte (1974) showed $Pe \gg 1$ for major orogenic belts; hence, synorogenic thermal conduction is negligible and crustal thickening may be regarded as instantaneous when thermal effects are concerned. Consequently, most thermal models approximate crustal thickening by instantaneous overthrusting of a crustal sheet onto the continental lithosphere, resulting in an initial sawtooth geotherm as shown in Fig. 5a. This sharp thermal gradient, however, would be smoothed quickly by thermal diffusion because, according to the Fourier's law, conductive heat flux is proportional to thermal gradient (Carslaw and Jaeger, 1959). This process, sometimes referred to as thermal relaxation, redistributes heat within the crust but cannot significantly raise the crustal temperature by itself. The increase of crustal temperature shown in Fig. 5a is mainly due to enhanced radioactive heating because of crustal thickening. Studies in many continental regions have shown that the concentration of heat-producing elements decreases exponentially with depth (Lachenbruch, 1970): $A(z) = A_0 \exp(-z/d)$, where $A(z)$ is volumetric radioactive heating at depth z and A_0 is the surface value, d is the characteristic decay length. Overthrusting of crustal sheets increases radioactive heating within the

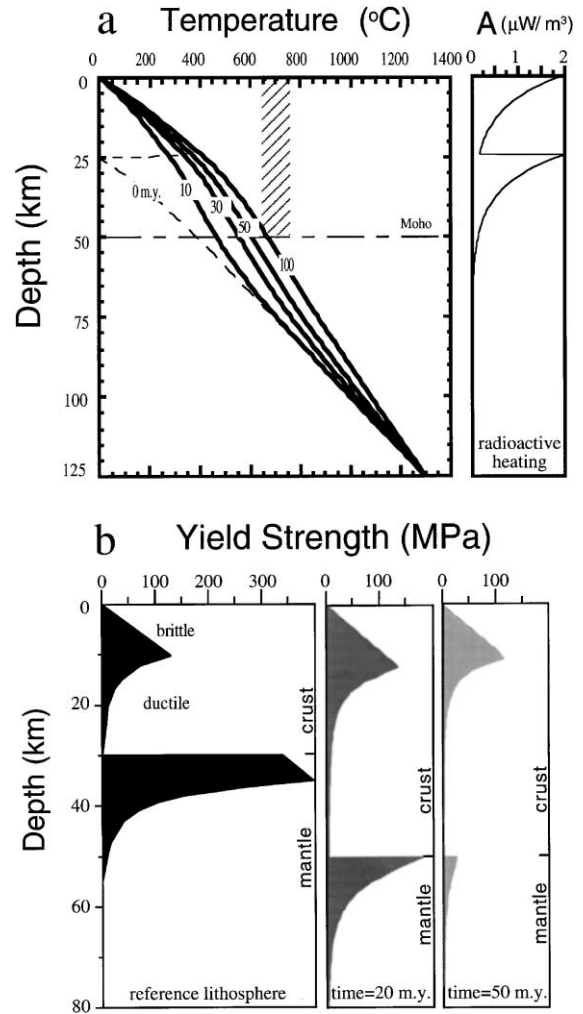


Fig. 5. (a) Thermal evolution within a model lithosphere following an instantaneous crustal thickening by stacking a 25-km crustal sheet. Boundary conditions are fixed temperature at the top (0 °C) and the base of the lithosphere (1350 °C), defined as the conductive lid. The hatched bar indicates the range of solidus of wet granitic rocks. The volumetric radioactive heating rate is $2 \mu\text{W}/\text{m}^3$ at the surface and decays exponentially with depth. The right panel shows the vertical distribution of radioactive heating after crustal thickening. (b) Strength envelopes of a model lithosphere. The left panel is for the reference lithosphere with a 30-km-thick granitic crust. The initial thermal structure is characterized by an equilibrium geotherm with a surface heat flux of $60 \text{ mW}/\text{m}^2$. The middle panel shows the strength 20 m.y. after an instantaneous crustal thickening. Reduction of the lithospheric strength is due to postkinematic thermal relaxation and radioactive heating and the mantle lithosphere being pushed to a deeper and warmer environment. The right panel shows the lithospheric strength after 50 m.y. of crustal thickening.

crust. The right panel in Fig. 5a shows the vertical distribution of $A(z)$ after crustal thickening.

The increasing temperature following crustal overthrusting (Fig. 5a) would weaken the lithosphere. The mechanical strength of the lithosphere can be shown by the strength envelope, defined as the minimal differential stress needed to cause brittle or ductile deformation at a given depth (Kusznir and Park, 1984; Lynch and Morgan, 1987; Ranalli and Murphy, 1987) (Fig. 5b). The yield stress for brittle deformation, $\sigma_b(z)$, depends primarily on pressure (Byerlee, 1978) and may be estimated as $\sigma_b(z) = \mu \rho g z$, where μ is the frictional coefficient (Liu and Furlong, 1993; Lynch and Morgan, 1987). The yield stress for ductile deformation, $\sigma_d(z)$, has a power-law relationship to the strain rate (Brace and Kohlstedt, 1980):

$$\sigma_d = \left(\frac{\dot{\epsilon}}{A} \right)^{1/n} \exp\left(\frac{H}{nRT} \right), \quad (5)$$

where $\dot{\epsilon}$ is the strain rate, A and n are material constants, H is the activation enthalpy, R is the gas constant, and T is the absolute temperature (see Table 2). Note that $\sigma_d(z)$ decreases exponentially as temperature increases.

Fig. 5b shows that the continental lithosphere typically has a jelly-sandwich rheological structure: a brittle upper crust, a ductile lower crust, and a strong uppermost mantle. The strength envelope varies with the temperature, thickness, and composition of the crust. Because olivine, the predominant mineral in the upper mantle, has a rheology highly sensitive to temperature (Karato et al., 1986; Kirby and Kronenberg, 1987), the lithosphere can be further weakened by crustal thickening that pushes the mantle lithosphere down to a deeper and hotter environment (Glazner and Bartley, 1985).

The total lithospheric strength can be measured by the vertical integral of yield stresses across the entire lithosphere (Kusznir and Park, 1984; Lynch and Morgan, 1987):

$$s = \int_l^0 \sigma_y(z) dz; \quad \sigma_y(z) = \min(\sigma_b(z), \sigma_d(z)), \quad (6)$$

where l is the base of the reference lithosphere. Fig. 6 compares the lithospheric strength and the gravitational buoyancy force of a model orogen where crust is thickened from 35 to 50 km by instantaneous

overthrusting of a crustal sheet. The gravitational buoyancy force is 3.5×10^{12} N/m from Eq. (3). To drive major extension, it has to overcome the lithospheric yield strength, which is a few times higher immediately after the instantaneous crustal thickening, depending on the initial thermal structure of the lithosphere. Thermal relaxation and radioactive heating, however, reduces $\sigma_d(z)$ and, thus, the lithospheric strength. Within 10–40 m.y., the yield strength is much smaller than the buoyancy force, and significant extension may be expected. This time interval required for sufficient thermal weakening of the lithosphere agrees generally with that between the end of crustal shortening and onset of crustal extension in the North American Cordillera (Wernicke et al., 1987). Similar thermal–rheological analysis has been applied to continental extension in many regions (Liu and Furlong, 1993; Lynch and Morgan, 1987; Ranalli et al., 1989; Sonder et al., 1987).

2.1.3. Postorogenic magmatism

In the North American Cordillera, the core-complex formation was closely correlated with plutonism

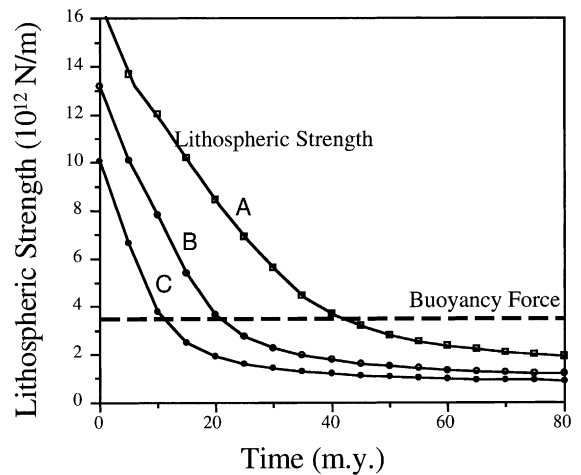


Fig. 6. Lithospheric weakening by thermal relaxation and enhanced radioactive heating associated with crustal thickening (see Fig. 5b). The three curves show the total yield strength of model lithospheres with different initial thermal structures characterized by an equilibrium surface heat fluxes of 47 (curve A), 55 (curve B), and 62 mW/m^2 (curve C). The total buoyancy force (dashed line) is calculated (see Eq. (3) in text) for a 50-km-thick crustal welt that is at Airy isostasy and surrounded by a 35-km-thick lowland crust.

(Armstrong, 1982; Wernicke et al., 1987). Similar relationship between extension and magmatism is common in orogens (Armstrong and Ward, 1991; Dewey, 1988; Glazner and Bartley, 1985). We have shown in Fig. 6 that gravitational collapse of orogens tends to occur where the crustal temperature is high, and plutonism can facilitate crustal extension by allowing localized ductile deformation in the otherwise brittle upper crust (Lister and Baldwin, 1993). The cause of the magmatism, however, remains uncertain.

Previous studies have suggested that postorogenic thermal relaxation and radioactive heating may cause major crustal anatexis (Glazner and Bartley, 1985; Zen, 1988). However, a constant mantle heat flux is often used as a boundary condition in these models (e.g., England et al., 1992; Zen, 1988). Liu and Furlong (1993) argued that the mantle heat flux would decrease as postorogenic thermal processes heating up the crust and reducing or even reversing the thermal gradient near the base of the crust. Using a constant mantle heat flux would lead to overestimation of crustal temperatures. Because of the transient geotherm in orogenic belts, a better boundary condition for thermal models is a constant temperature at the base of the conductive lid (the thermal boundary layer) that may be maintained by convective circulation in the asthenosphere (Parsons and McKenzie, 1978). Using this thermal boundary condition, we have shown that postorogenic thermal relaxation and radioactive heating usually are insufficient to cause major crustal anatexis (see Fig. 5a).

One solution is to have a high concentration of heat-producing elements in the crust. Accretion and

erosion in collisional orogens may produce a wedge with high concentration of heat-producing elements (Huerta et al., 1998; Jamieson et al., 1998). Fig. 7a shows the thermal evolution when the rate of radioactive heating is doubled ($A_0 = 4 \mu\text{W}/\text{m}^3$). In this case, major anatexis in the middle to lower crust is

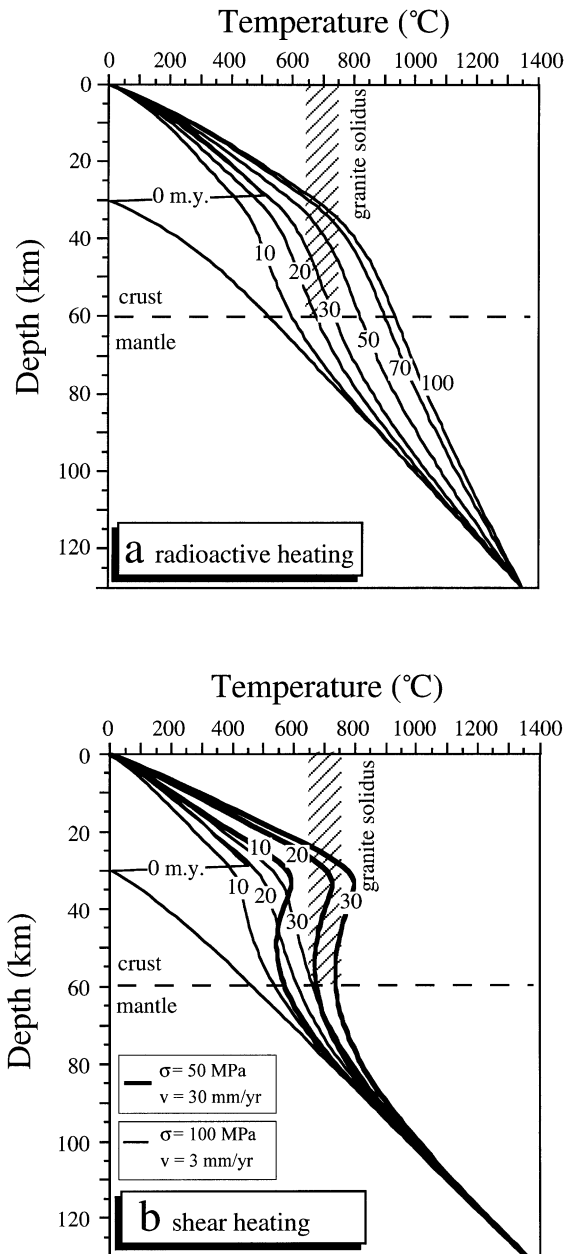


Fig. 7. (a) Effects of enhanced radioactive heating. The initial lithosphere is 100-km thick with a 30-km-thick crust, which was instantaneously doubled to 60 km by overthrusting of a 30-km crustal sheet. The boundary conditions are fixed temperature at the surface (0°C) and the base of the lithosphere (1350°C). The radioactive heating is $4 \mu\text{W}/\text{m}^3$ at the surface, twice as much as that in Fig. 5a. Crustal thickening causes stacked radioactive layers as those in Fig. 5a. The hatched bar shows the minimum solidus for wet granitic crust. (b) Effects of shear heating. Parameters differing from those in (a) are $A_0 = 2 \mu\text{W}/\text{m}^3$ and inclusion of shear heating along the interface of crustal doubling. Shear heating declines from the interface in a Gaussian fashion with a characteristic length of 5 km. The thick and thin curves are results of two cases with different shear stresses and thrusting rates as indicated in the figure.

predictable. However, we will show below that a high concentration of heat-producing elements in the crust is not supported by observations from the Cordillera.

Another possible heat source for orogenic magmatism is shear or frictional heating (England and Molnar, 1993; Harrison et al., 1998; Molnar and England, 1990; Nabelek and Liu, 1999b). Shear heating has been an issue of controversy because of the uncertainty of shear stresses in thrusting zones and the problem of self-regulation of shear heating (Yuen et al., 1978). For a first-order approximation, the rate of shear heating, A_s , may be estimated assuming a constant shear stress (Harrison et al., 1998; Shi and Zhu, 1993): $A_s = v\sigma/\delta z$, where σ is the shear stress, v is the velocity of shearing, and δz is the thickness of the shearing zone. Some studies have assumed high shear stresses (>100 MPa) for major orogenic thrusting faults (England and Molnar, 1993; Molnar and England, 1990); others have shown that moderate shear stresses (30–50 MPa) are sufficient to produce major crustal partial melting (Harrison et al., 1997, 1998; Nabelek and Liu, 1999a). One factor that has not received enough attention is the velocity of shearing. Fig. 7b shows that shear heating can cause significant partial melting within the middle to lower crust for a shear stress of 50 MPa and a thrusting velocity of a few centimeters per year. However, when the shearing velocity is on the order of a few millimeter per year, as was suggested for crustal contraction during the Cordilleran orogeny (Elison, 1991), the effects of shear heating are limited even when shear stresses >100 MPa are used (see Fig. 7b).

Notice that in Figs. 5a and 7, the geotherms were initially depressed, because the conductive lid is thickened following crustal thickening. A thickened conductive lid (the thermal boundary layer) is unstable and may induce downwelling mantle flow (Houseman et al., 1981), causing thinning of the lithosphere and, therefore, significant mantle thermal perturbations (England, 1993). Heat advected by mantle upwelling can cause major crustal anatexis. Fig. 8 shows two end-member cases of mantle upwelling. One is for an instantaneous mantle upwelling followed by conductive cooling (Fig. 8a); the other is to have a constant potential temperature of the upwelling mantle, presumably main-

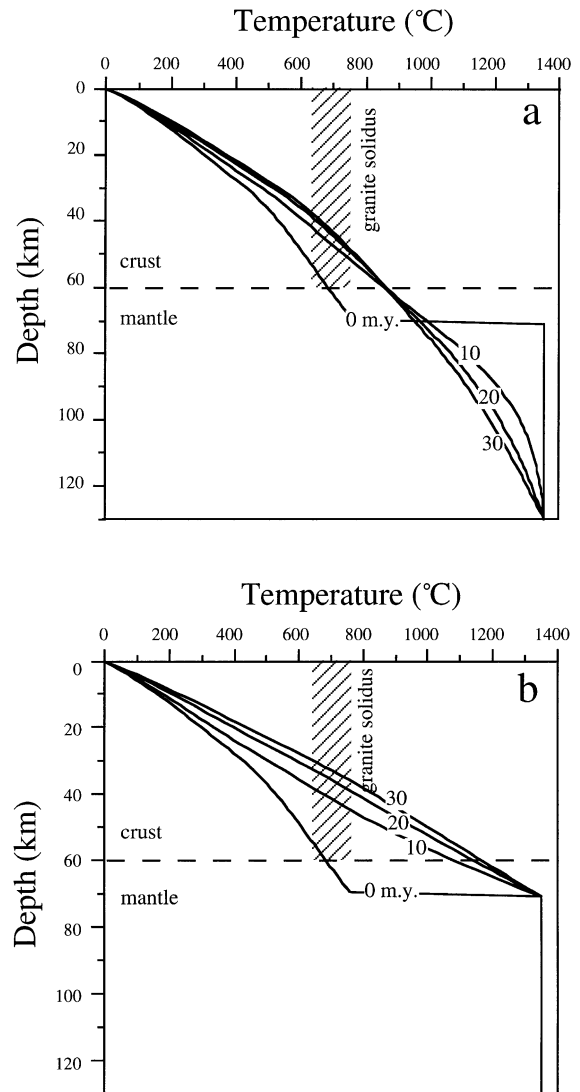


Fig. 8. Thermal effects of mantle upwelling. (a) Instantaneous upwelling of the asthenosphere with a constant temperature of 1350 °C to 70-km depth, followed by conductive cooling. The boundary condition includes a fixed temperature at the surface (0 °C) and at 130 km, the initial depth of the lithospheric base (1350 °C). The hatched bar shows the minimum solidus for wet granitic crust. (b) Temperature within the upwelled asthenosphere is maintained at 1350 °C after the asthenospheric upwelling.

tained by vigorous small-scale convection. In both cases, significant crustal anatexis is predictable, especially when the temperature in the upwelling mantle can be maintained by convective heating

(Fig. 8b). The dynamic effects of mantle upwelling on gravitational collapse are discussed later in this paper.

2.1.4. Gravitational spreading of a thickened crust

Although the link between synorogenic and post-orogenic extension is not clear, the later is expected to be significantly different from the former because of its association with high crustal temperature and magmatism. Specifically, crustal thickening and postorogenic thermal processes tend to produce a thick and weak ductile lower crust (see Fig. 5b); thus, postorogenic gravitational collapse may be largely accommodated by ductile spreading. Ductile flow under a thickened crust is believed to have played an important role in the North American Cordillera and other orogens, and has been investigated in models of plane channel flow (Bird, 1991; Block and Royden, 1990; Hopper and Buck, 1996; Kruse et al., 1991). The channel flow model assumes that ductile flow within the lower crust is mechanically decoupled from the mantle lithosphere. This is a reasonable assumption for typical continental lithosphere, because the uppermost mantle is usually the strongest layer within the lithosphere (see Fig. 5b), and shear stress exerted on the mantle lithosphere by ductile crustal flow is limited (Liu and Shen, 1998a). However, under orogenic belts, the mantle lithosphere can be sufficiently weakened by postorogenic thermal processes that it may flow together with the ductile crust. Whether or not this process can lead to whole-lithospheric extension and significant mantle upwelling is critical for understanding the dynamic links among core-complex formation, mid-Tertiary volcanism, and basin-and-range extension.

We investigate gravitational ductile spreading under a crustal welt in a two-dimensional ductile flow model assuming full mechanical coupling between the crust and the mantle. Fig. 9a shows the model geometry and boundary conditions. The crustal welt is produced by an instantaneous crustal thickening from 34 to 50 km. The initial thermal structure of the lithosphere is characterized by a steady-state surface heat flux of 60 mW/m^2 . The topography of the crustal welt is not shown in the figure but included in the calculations. For typical geological strain rate (10^{-14} – 10^{-17} s^{-1}), the inertia term can be neg-

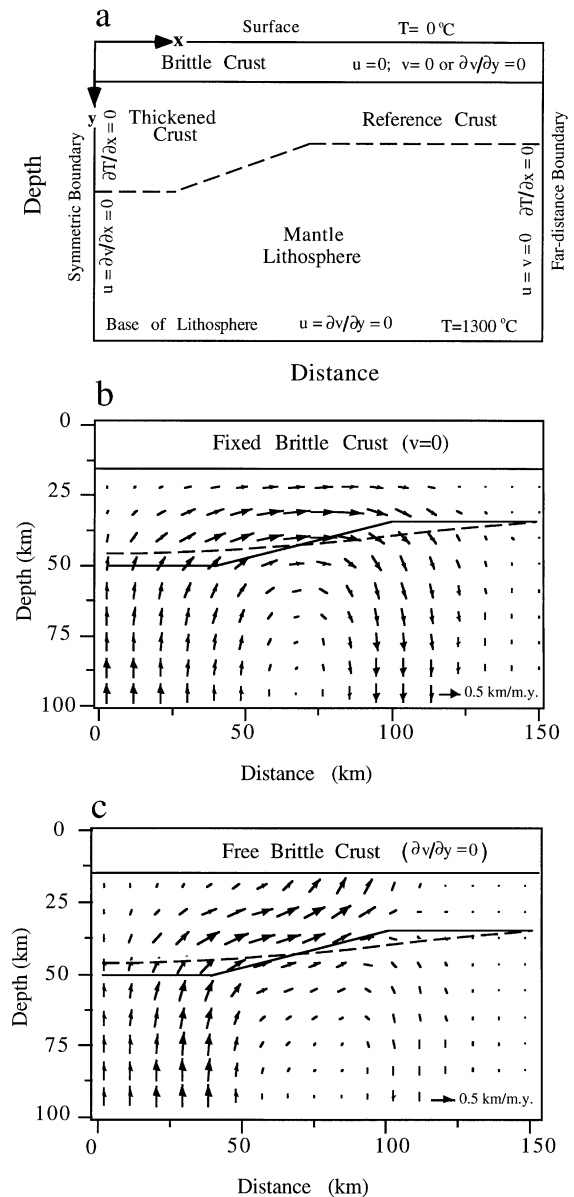


Fig. 9. (a) Model of gravitational collapse of a crustal welt by ductile spreading. Brittle deformation is not included. The left side is a symmetric boundary; the right side is a far-distance boundary. Topographic head of the crustal welt is not shown but included in the calculations. (b) Snapshot of the velocity field at 12 m.y. after an instantaneous crustal thickening from 34 to 50 km. The dashed line indicates the Moho whose initial location is shown by the solid line. A rigid top boundary ($u=v=0$) is assumed. (b) Same as (a) but the top boundary is vertically free ($u=\partial v/\partial y=0$).

lected from the momentum equation, which takes the general form

$$\frac{\partial p}{\partial x_i} = \frac{\partial \sigma_{ij}}{\partial x_j} - \rho \vec{g}; \quad (i, j = x, y), \quad (7)$$

where p is the pressure, σ_{ij} is the stress tensor, and \vec{g} is the vector of gravitational acceleration. For the

crustal structure in Fig. 9a, ductile spreading is driven by the lateral pressure gradient between the thickened crust and surrounding lowland (see Fig. 3):

$$\frac{\partial p}{\partial x} = \rho_c g \frac{\partial h_r}{\partial x}, \quad (8)$$

where $\partial h_r / \partial x$ is the topographic gradient assuming constant crustal density ρ_c . To isolate the effects of gravitational spreading, the right side of the model is taken to be a fixed boundary with no stretching or compression imposed. In the calculations, this boundary is also taken to be a far-distance boundary, where its effects on the flow field are proven negligible. The power-law flow rheology of the ductile crust expressed in Eq. (5) can be rewritten as (England and McKenzie, 1982; Shen, 1997):

$$\sigma_{ij} = B \dot{E}^{(1/n-1)} \dot{\epsilon}_{ij}, \quad (9)$$

where $\dot{\epsilon}_{ij}$ is the strain rate tensor defined as

$$\dot{\epsilon}_{ij} = \frac{1}{2} \left(\frac{\partial u_i}{\partial x_j} + \frac{\partial u_j}{\partial x_i} \right), \quad (10)$$

and \dot{E} is the second invariant of the strain rate tensor. The coefficient B is defined as

$$B = A^{-1/n} \exp\left(\frac{H}{nRT}\right). \quad (11)$$

Rheological parameters used in this study are given in Table 2. Substituting Eq. (9) into Eq. (7) and

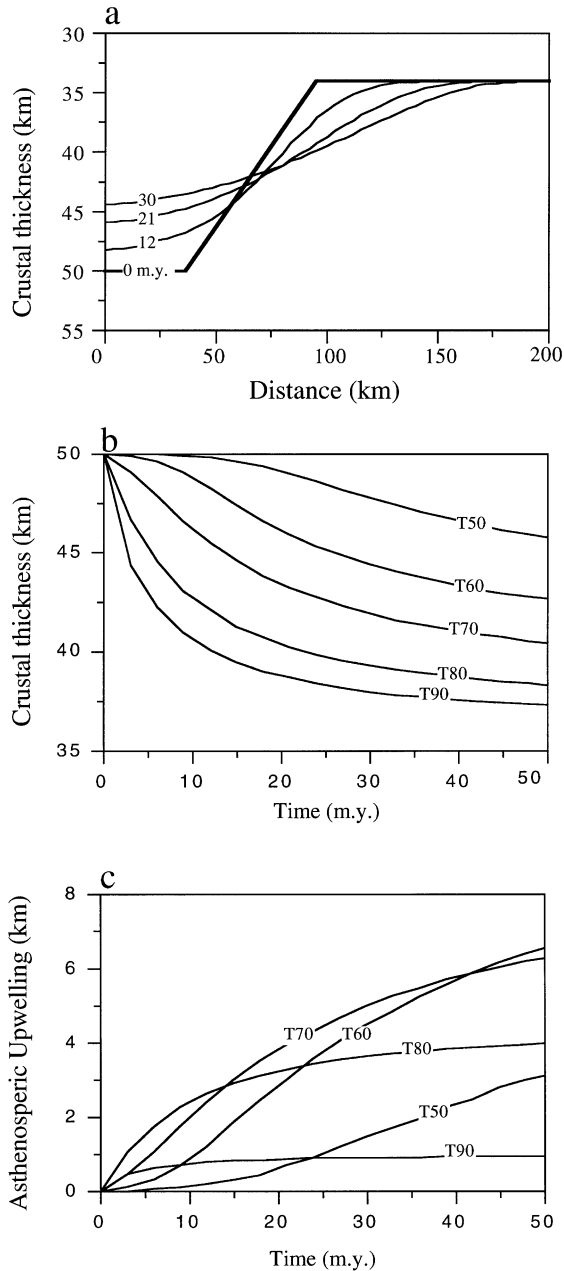


Fig. 10. (a) Thinning of a crustal welt by ductile spreading. Initial geotherm of the lithosphere is characterized by a steady-state surface heat flux of 60 mW/m². Time is after ductile spreading started. Other conditions are the same as in Fig. 9b. (b) Effects of initial thermal structures on ductile spreading. The curves show the maximum thinning of a crustal welt by ductile spreading at different time. The curve labeled T40 is the result with an initial geotherm characterized by a steady-state surface heat flux of 40 mW/m²; same meaning applies to other curves. Time is after ductile spreading started. (c) Time integrated thinning of the lithosphere induced by ductile spreading of the crustal welt. The curves show results with different initial thermal structures explained in (b). Calculated by integrating the vertical mass flux in the ductile flow model (see Fig. 9b).

using Eq. (8), the velocity field of the ductile flow can be derived as (Shen, 1997):

$$\begin{aligned} \nabla^2 \vec{u}_i = & -\frac{\partial D}{\partial x_i} + \frac{2}{B} \dot{E}^{(1-1/n)} \frac{\partial P}{\partial x_i} \\ & + 2 \left(1 - \frac{1}{n}\right) \dot{E}^{-1} \frac{\partial \dot{E}}{\partial x_j} \dot{\epsilon}_{ij} \\ & + \frac{2Q}{nRT^2} \frac{\partial T}{\partial x_j} \dot{\epsilon}_{ij}, \end{aligned} \quad (12)$$

where $\vec{u} = (u, v)$ is the velocity vector, $P = p - \rho gy$ is the pressure with the lithostatic component removed, and $D(x, y) = \partial u_i / \partial x_i = 0$ is a function used to enforce volume conservation in the numerical scheme.

Fig. 9 shows snapshots of the predicted flow field of ductile spreading at 12 m.y. after the initial crustal thickening. The top boundary of the model is free in Fig. 9a and rigid in Fig. 9b. These two end-member cases should bracket the response of the upper crust to ductile deformation in the lower crust. In both cases, the lateral extrusion of ductile material, as indicated by the horizontal flow, is concentrated within the lower crust. The greatest flow rates are found near the margins of the crustal welt where the lateral pressure gradient is the highest. The vertical flow is passively induced by the lateral flow as required by volume conservation.

Some of the dynamic effects of the ductile spreading with a fixed top boundary (Fig. 9b) are shown in Fig. 10. The results with a free top boundary are not significantly different. Fig. 10a shows the flattening of a model crustal welt by ductile spreading. In all experiments, the rate of flattening decreases quickly with time because the lateral pressure gradient is reduced during ductile spreading. The flow is slower when the rheology of granite is replaced by that of diabase (see Table 2), but the general results are the same. As shown by previous studies (Bird, 1991), the rate of ductile spreading is sensitive to crustal temperature. Fig. 10b shows the thinning of the crustal welt

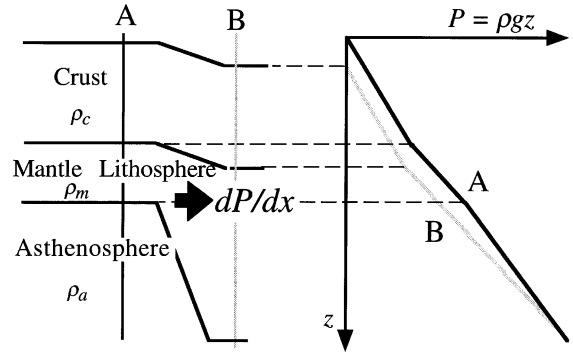
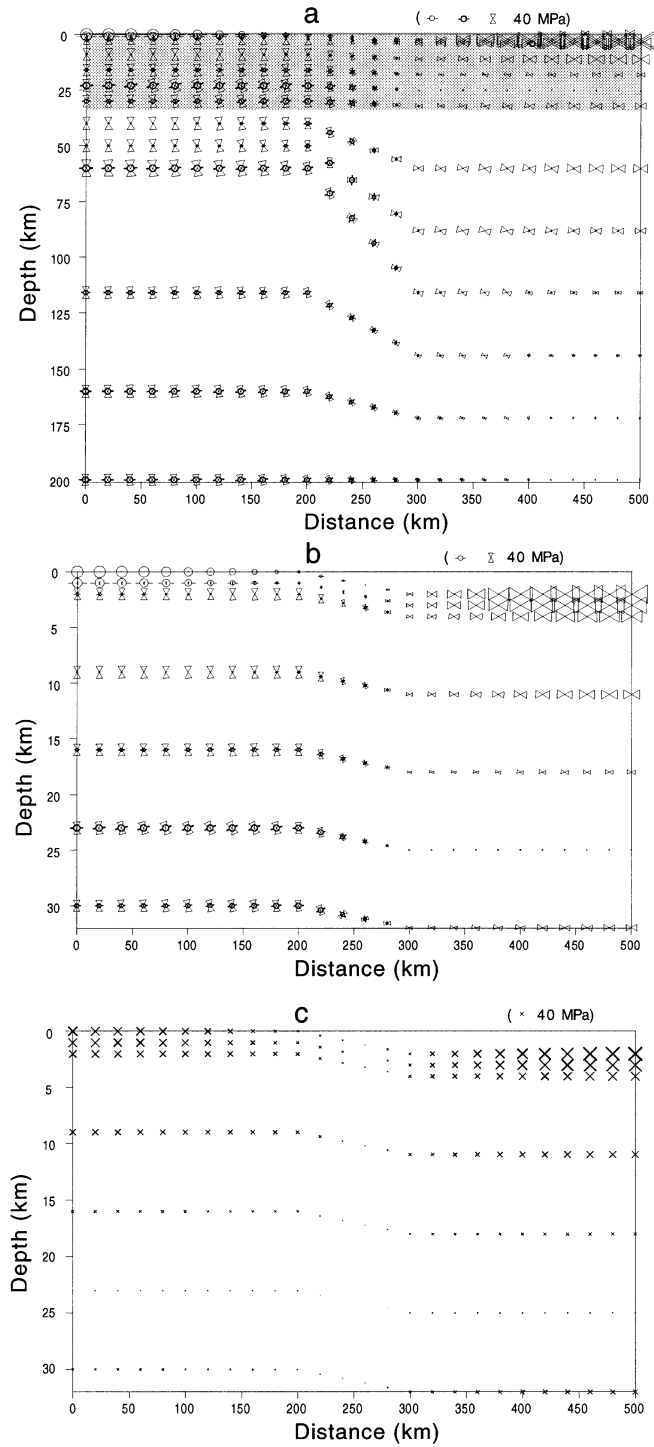


Fig. 11. Sketch showing a topographic head isostatically supported by an upwelling asthenosphere (left). Lithostatic pressure profiles in region of upwelling asthenosphere (A) and adjacent lowland (B) (right). Parameters ρ_c , ρ_m and ρ_a are density of the crust, mantle, and asthenosphere, respectively ($\rho_c < \rho_a < \rho_m$). Note that although lithosphere is at isostatic equilibrium, pressure along profile A is greater than that along B at any given depth above the base of the reference lithosphere. The lateral pressure gradient tends to drive ductile flow within the surrounding lithosphere.

with time when we use different initial lithospheric thermal structures, characterized by different steady-state surface heat fluxes. For most orogens, the crustal root will be largely removed within 20 Ma by ductile spreading within the lower crust.

One question important for the Cordilleran tectonics is whether or not gravitational collapse of the thickened crust can induce major asthenospheric upwelling. The amount of asthenospheric upwelling induced by crustal spreading can be calculated by integrating the induced vertical mass flux (Shen, 1997). Fig. 10c shows that the amount of asthenospheric upwelling increases with the initial temperature of the lithosphere, because the rate of ductile spreading is temperature-dependent. However, further increase of crustal temperature would cause less mantle upwelling, because the effective viscosity of the lower crust is reduced by increasing temperature, which results in a weaker coupling between the mantle and the crust (Liu and Shen, 1998a). In any

Fig. 12. (a) Non-lithostatic stresses within a model lithosphere with asthenospheric upwelling to 60-km depth. The crust has a uniform thickness of 30 km. A 2-km plateau (not shown in the figure) is supported by the upwelling mantle, which has a 100 kg/m³ density deficiency relative to the reference mantle. The boundary conditions are similar to those in Fig. 4. The top 30 km is elastic media, the rest assumes a temperature-dependent power-law flow rheology (see text). Only the left half of the model is shown because of symmetry. Stress symbols are explained in Fig. 4. The gray block is enlarged in (b) and (c). (b) Principal non-lithostatic stresses within the crust showing extensional stress states within the plateau and compressional regions within the lowland. (c) Differential stresses ($|\sigma_1 - \sigma_2|$) within the crust.



case, the amount of asthenospheric upwelling induced by crustal spreading is limited (<10 km). Thus, postorogenic gravitational collapse of thickened crust alone is unlikely to lead to major whole-lithospheric extension.

2.2. *Gravitational collapse of orogens over an upwelling asthenospheric mantle*

Similar to crustal thickening, asthenospheric mantle upwelling also provides excess gravitational potential energy to drive orogenic extension. England and Houseman (1989) suggested that mantle upwelling under the northern Tibetan plateau has played a major role in the uplift and extension of the plateau. The present extension in the Basin and Range is believed to be driven mainly by the buoyancy force from an abnormally hot upper mantle (Jones et al., 1996; Sonder and Jones, 1999).

Fig. 11 shows that, when a topographic head is supported by thermal buoyancy force in the upwelling asthenosphere, a lateral pressure gradient is induced across the entire lithosphere that tends to cause lithospheric extension in a way similar to that associated with a thickened crust (compare to Fig. 3). We have calculated the stress state of the lithosphere over an upwelling asthenospheric mantle (Fig. 12). Within the top 15 km under the plateau, the stress states are extensional as indicated by the nearly vertical σ_1 . The differential stress, $|\sigma_1 - \sigma_2|$, is > 50 MPa in the upper crust; thus, significant normal faulting is predictable. Notice that a fixed right-side boundary is used here.

The predicted crustal extension is more extensive when we use a displacement boundary that reflects regional extension.

Asthenospheric mantle upwelling can also cause significant ductile spreading within the surrounding lithosphere, because the lateral pressure gradient is non-zero across the entire lithosphere, and heat advected by the upwelling mantle could effectively soften the surrounding lithosphere. Fig. 13a shows the numerical model we used to simulate ductile spreading within the lithosphere induced by asthenospheric

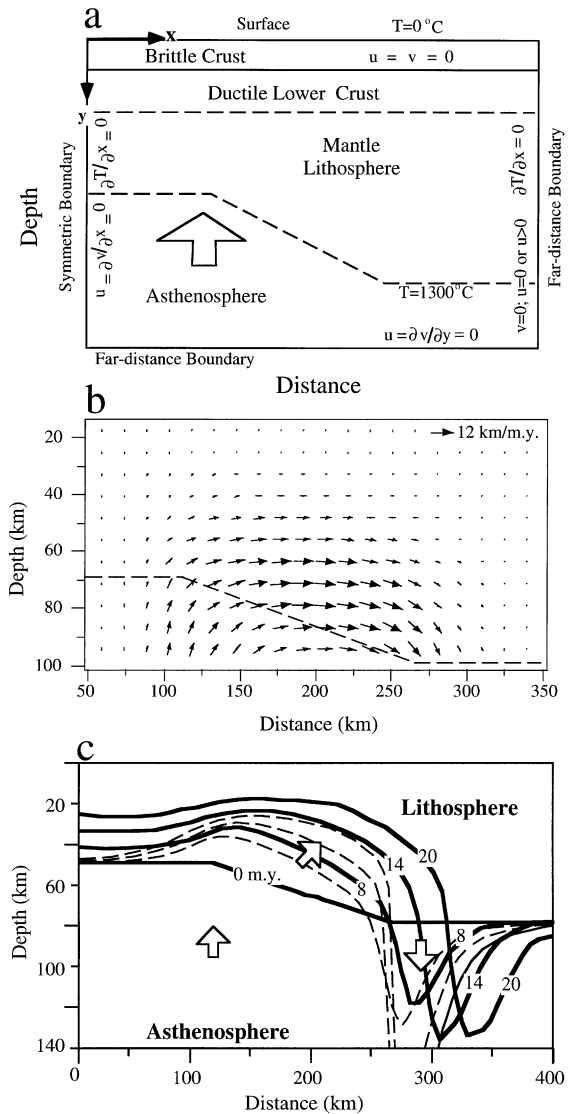


Fig. 13. (a) Model of ductile spreading induced by asthenospheric upwelling. The right side is either a neutral ($u=0$) or a uniform stretching ($u=5$ mm/year) boundary. (b) Predicted ductile flow induced by the lateral pressure gradient illustrated in Fig. 11. Asthenospheric upwelling is assumed to be instantaneous, and a constant temperature (1300°C) is held at the initial lithosphere–asthenosphere boundary (dashed line). Showing here is only part of the model domain near the upwelling asthenosphere. The left side of the model is a symmetric boundary, and the right side (at distance=500 km, not shown) is a fixed far-distance boundary where flow velocity and lateral heat transfer are negligible (see Liu and Shen, 1998b for details). (c) Time-integrated thinning of mantle lithosphere near the upwelling asthenosphere resulting from the ductile flow in (b). Solid curves are the results with 5 mm/year stretching imposed on the right side of the model, and dashed curves are results with $u=0$ on the right side boundary. Arrows indicate general pattern of ductile flow induced by mantle upwelling.

upwelling. The model geometry and boundary conditions are similar to those in Fig. 9a for a thickened crust, except in this case the lateral pressure gradient is induced by the buoyant upwelling asthenosphere. Fig. 13b is a snapshot of the predicted flow field. The lateral pressure gradient between the thermally perturbed lithosphere and the surrounding regions (see Fig. 11) pushes the lithospheric material to flow away and downward, causing the asthenosphere to gradually replace the mantle lithosphere (Fig. 13c). Most thinning of the lithosphere occurs near the margins of the upwelling asthenosphere where the pressure gradient is the greatest. If a regional extension is imposed on the model, the loci of maximum lithospheric thinning would migrate away from the center of mantle upwelling. We show below that this migration of mantle thermal perturbations may have useful implications for the temporal–spatial evolution of late Cenozoic volcanism in the Great Basin.

3. Gravitational collapse in the Cordillera: geodynamic constraints

The thermal–rheological and thermomechanical modeling of gravitational collapse of orogens discussed above may provide useful constraints for geodynamic evolution of extension and magmatism in the North American Cordillera. Here, we apply these results to discuss the roles and limitations of gravitational collapse in core-complex formation and plutonism, the mid-Tertiary volcanism, and basin-and-range extension.

3.1. Core-complex formation and the associated plutonism

The formation of metamorphic core complexes marks the onset of postorogenic extension in many regions of the North American Cordillera. Although the cause of metamorphic core complexes remains debatable, many workers have emphasized the role of gravitational collapse of the thickened crust of the Cordilleran orogen (Coney and Harms, 1984; Liu and Shen, 1998a; Livaccari, 1991; Sonder et al., 1987; Vanderhaeghe and Teyssier, 1997). Our results support a major role of gravitational collapse in the core-complex formation. We have shown that the thickened

crust (>50 km, see Coney and Harms, 1984; Parrish et al., 1988) in the Cordilleran orogen was dynamically unstable, and thermal processes associated with crustal thickening may have sufficiently weakened the crust. Thus, major gravitational collapse of the Cordilleran orogen is predictable (see Figs. 3–6). Furthermore, we conclude that gravitational collapse of the thickened crust of the Cordilleran orogen was largely accommodated by ductile spreading in the middle–lower crust. The crust was not only thick but also abnormally warm when core complexes formed, as indicated by the overlapping plutonism (Armstrong and Ward, 1991). Wernicke et al. (1987) and Parrish et al. (1988) showed that temperature in the middle to lower crust was >700 °C when core complexes formed. For a thick and warm crust, the ductile rheology becomes predominant (see Fig. 5b), and ductile spreading becomes an effective way of gravitational collapse (see Figs. 9 and 10). The high rates of ductile spreading in a hot crust predict relatively short life span of core-complex formation. Fig. 14 is one example comparing the gravitational buoyancy force with the yield strength of the lithosphere during ductile spreading. The results are calculated in a ductile flow model similar to that described

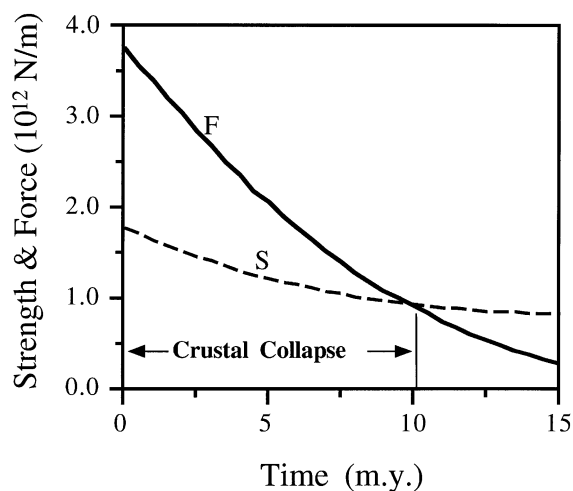


Fig. 14. Evolution of the total buoyancy force (F) and the yield strength of the lithosphere (S) during gravitational collapse of a crustal welt dominated by ductile spreading in the lower crust (see Fig. 9). Time is after the initiation of gravitational collapse, which is expected to stop within ~ 10 Ma when $F < S$.

in Fig. 9. The crustal welt is initially 55-km thick, and the ductile spreading is allowed to start when the temperature near the base of the crust reaches 700 °C by thermal relaxation and radioactive heating. At the onset of ductile spreading, the gravitational buoyancy force arising from the thickened crust is nearly twice as much as the yield strength of the lithosphere. However, it reduces quickly as the crustal welt being thinned by ductile spreading, while the lithospheric yield strength reduces slightly due to the competing effects of crustal thinning and enhanced cooling by extension that tends to harden the crust. When the driving force is less than the yield strength, the process is expected to end. For high crustal temperatures suggested by thermochronological data from the core complexes (Parrish et al., 1988; Wernicke et al., 1987), ductile spreading has a typical life span of 10–15 m.y., which is consistent with the life span associated with many core complexes in the Cordillera (Parrish et al., 1988).

For the plutonism that overlapped core-complex formation over time and space in the Cordillera, the heat sources necessary for their generation remain uncertain. We have shown that postorogenic thermal relaxation takes 30–50 m.y. to heat up the crust (Fig. 5a), whereas in the southeastern Canadian Cordillera major crustal extension started a few million years after the end of crustal shortening (Parrish et al., 1988). Liu and Furlong (1993) argued that, because crustal shortening in the Cordillera was a long (165–55 Ma) and slow (<5 mm/year) process, synorogenic heat conduction cannot be ignored as in models of instantaneous crustal thickening, but should be integrated through the entire history of crustal thickening. Nonetheless, additional heat source is needed, because thermal relaxation alone is inadequate to produce major crustal anatexis (see Figs. 5a and 7a). Higher crustal temperature can be predicted by assuming higher concentration of radioactive elements within the crust or slower decay of their concentration with depth. The value of radiogenic heating used in Fig. 5a, $A_0 = 2 \mu\text{W}/\text{m}^3$, is a typical value for continental crust. There is no evidence for either a much higher concentration of radioactive elements or a thicker radioactive layer in the Cordillera. Lachenbruch et al. (1994) and Sass et al. (1994) showed that the typical values of A_0 for the Cordilleran crystalline crust is $2.1 \mu\text{W}/\text{m}^3$, which is reduced to $1.3 \mu\text{W}/\text{m}^3$ in the middle

crust. Another possibility is frictional or shear heating, which can be effective in causing partial melting within the middle crust if thrusting was at a rate of a few centimeters per year. For the average slow rate of crustal shortening in the Cordillera (<5 mm/year) (Elison, 1991), the effects of shear heating may be limited (Liu and Furlong, 1993) (see Fig. 7b). It seems that in some regions, especially the southeastern Canadian Cordillera, where major extension and plutonism followed the end of crustal shortening within a few million years, some mantle thermal perturbation was needed (Liu and Furlong, 1993; Ranalli et al., 1989). The role of mantle thermal perturbation is suggested by intrusion of mafic dykes in some core complexes (Armstrong, 1982), and by the lens-shaped velocity structures under some metamorphic core complexes that are suggestive of mixture of mafic and silicic magmas (McCarthy et al., 1991). As we have shown in Fig. 8, even moderate mantle upwelling can cause significant crustal partial melting. On the other hand, the spatially and temporally restricted crustal extension related to core-complex formation in the Cordillera do not support a large-scale, widespread mantle upwelling at this time.

3.2. *Mid-tertiary magmatism and extension in the Great Basin*

South of the Snake River plain, intensive eruption of silicic volcanic rocks overlapped or followed the formation of core complexes (Armstrong, 1982; Armstrong and Ward, 1991; Coney, 1987; Wernicke et al., 1987). The relationship between this silicic volcanism and core-complex formation remains controversial. Previous studies have related this mid-Tertiary volcanism to a southward foundering of the subducting Farallon plate, because the geochemical signatures of these volcanic rocks are similar to those of subduction-related calc-alkaline suites of the Pacific rim (Lipman, 1980; Lipman et al., 1972). This interpretation, however, is inconsistent with a generally northward migration of magmatism in the southern Basin and Range (Glazner and Bartley, 1984) (see Fig. 2b). Some recent studies have disputed the genetic link between subduction and the mid-Tertiary magmatism and instead argued that the geochemical signatures of these calc-alkaline volcanic rocks can be explained by extension-induced decompressional partial melting of

the mantle lithosphere that was enriched in incompatible elements since the Proterozoic (Hawkesworth et al., 1995; Hooper et al., 1995).

Our results do not support a direct link between gravitational collapse of the Cordilleran orogen and the voluminous mid-Tertiary volcanism. The problem with previous extension models is their difficulty of producing sufficient partial melting of mantle material. Significant intrusion and underplating of mafic magma were necessary to provide heat for the extensive crustal anatexis (Hildreth, 1981) and source materials for some of the silicic tuff (Grunder, 1995; Johnson, 1991). However, as shown in Fig. 15, peridotite mantle with a typical potential temperature of 1280 °C (1350 °C at the base of model lithosphere, see McKenzie and Bickle, 1988) needs to be brought up adiabatically to <50-km depth before significant decompressional partial melting could occur. This would require a stretching factor $\beta > 2$, or equivalently, more than 32 m.y. of pure-shear stretching at a constant strain rate of 10^{-15} s^{-1} , an upper limit of averaged strain rate in the Great Basin (Sonder and Jones, 1999). Our results show that this amount of mantle upwelling cannot be induced by gravitational collapse of the thickened crust in the Cordillera. The maximum asthenospheric upwelling induced by gravitational collapse of the thickened crust was <10 km

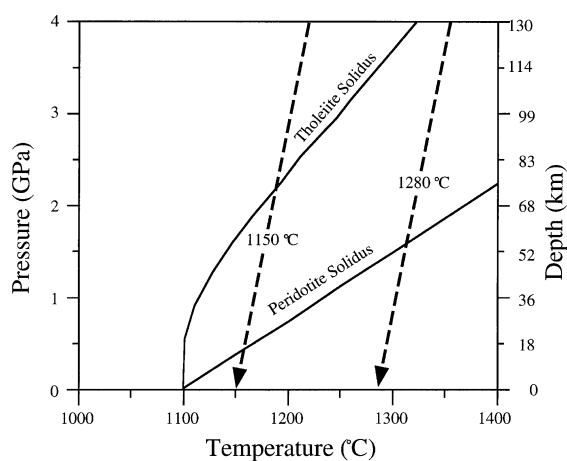


Fig. 15. Solidi for dry peridotite (McKenzie and Bickle, 1988) and tholeiite (Thompson, 1975). Dashed lines are the adiabatic paths for solid mantle material with the indicated potential temperatures. Depth is converted from pressure, assuming a 40-km-thick crust and density values in Table 1.

(see Fig. 10c), too small to cause major decompressional partial melting of the peridotite mantle. Harry and Leeman (1995) addressed this problem by proposing a metasomatized mantle as the protoliths of the mafic magma. Because the metasomatized mantle is expected to have a solidus somewhere in between those of peridotite and tholeiite (Fig. 15), significant partial melting may result from moderate lithospheric extension. Their model explains the isotopic signatures of mantle lithosphere in mid-Tertiary mafic volcanic rocks, and it predicts the observed decline of magma production after volcanic culmination in mid-Tertiary. However, their model cannot be readily reconciled with magmatism in many regions that was concurrent or predating extension (see review by Metcalf and Smith, 1995). Furthermore, most mid-Tertiary extension was localized and supracrustal; there is no evidence of significant extension of the whole lithosphere at that time.

One alternative is to have an active asthenospheric upwelling that can provide the needed thermal perturbations without requiring major lithospheric extension. The possible cause of active asthenospheric upwelling may include foundering or rollback of the subducting Farallon plate, delamination or convective downwelling of the thickened and thus unstable mantle lithosphere, a slab window, or mantle plume (see Liu and Shen, 1998a and references therein). Whatever the cause is, the voluminous mid-Tertiary volcanism in the Great Basin indicates strong mantle thermal perturbations. A strong mantle upwelling may also help to explain the apparent lack of spatial and temporal correlation between mid-Tertiary magmatism and extension. Numerous workers noted that the peak volcanism in central Great Basin between 34 and 17 Ma was accompanied by limited extension, and that most basin-and-range extension occurred ~ 10 m.y. after the peak silicic volcanism. Furthermore, the young basin-and-range extension was concentrated near the margins of the main volcanic field in central Great Basin, not within the volcanic field where the lithosphere was expected to be warm and weak (Axen et al., 1993; Best and Christiansen, 1991; Taylor et al., 1989). Liu and Furlong (1994) explained this temporal–spatial patterns of magmatism and extension in the Great Basin by the competing effects of thermal weakening and rheological hardening associated with intrusion and underplating of mafic

magma. Their results showed that the lithospheric strength derives mainly from that of the crust when asthenospheric upwelling significantly softens the mantle lithosphere. In this case, the lowest lithospheric strength occurs 5–10 m.y. after intrusion and underplating of mafic material associated with the peak mid-Tertiary volcanism. This time interval is for heat diffusion to weaken the crust following the mafic intrusion. However, by this time, the crust in the main volcanic fields may become stronger than the surrounding areas because of the added mafic material, which is stronger than felsic crustal material. Thus, when basin-and-range extension started, it concentrated near the margins of the main volcanic field where the crust was the weakest.

3.3. Basin-and-range extension and mantle upwelling

The cause of basin-and-range extension has been an issue of intensive studies and debate (e.g., Coney, 1987; Eaton, 1982; Stewart, 1978; Wernicke, 1992; Zoback et al., 1981). Our results may help to answer the question of whether or not basin-and-range extension resulted directly from gravitational collapse of the Cordilleran orogen, or more specifically, whether it is directly related to the earlier crustal extension associated with core-complex formation.

It was shown in some models (Harry et al., 1993) and implied in others (e.g., Sonder et al., 1987) that gravitational collapse of thickened crust would lead to basin-and-range extension. However, in the Cordillera, core-complex formation was not always followed by basin-and-range extension: Whereas core complexes occurred from southern Canadian cordillera to northern Mexico, basin-and-range extension is largely limited to the south of the Snake River Plain (see Fig. 2). There are also significant difference of extension and volcanism between the northern and southern Basin and Range province, indicating different stress fields and perhaps different causes (Glazner and Bartley, 1984; Sonder and Jones, 1999; Spencer et al., 1995; Wernicke, 1992). The fundamental features of basin-and-range extension in the Cordillera include significant whole-lithospheric extension and asthenospheric mantle upwelling. Significant mantle upwelling beneath the present Great Basin is indicated by the thin (~65 km) lithosphere (Smith et al., 1989), gravity anomalies (Eaton et al., 1978) and high heat

flow (Lachenbruch and Sass, 1978). Although the history of mantle upwelling beneath the Basin and Range is not well constrained, the continued extension and volcanism in the Great Basin (Lipman, 1980) indicate a major mantle upwelling since mid-Tertiary when volcanism in this region culminated. Liu and Shen (1998a) suggested that this asthenospheric upwelling may have set the stage for basin-and-range extension by providing the excess gravitational potential energy and by thermally weaken the lithosphere. In other words, basin-and-range extension may have resulted largely from gravitational collapse (Jones et al., 1996). However, in contrast to gravitational collapse of the thickened orogenic crust that led to core-complex formation, this young phase of gravitational collapse is driven by asthenospheric upwelling, and our results suggest that this asthenospheric upwelling was not directly induced by core-complex formation.

Although the cause of the asthenospheric upwelling under the Basin and Range province remains speculative, Liu and Shen (1998a) argued that the continued extension in the northern Basin and Range province over the past 20 Ma requires convective heating within the upwelled mantle to replenish heat lost through conduction, which is evident from the high heat flow in the Basin and Range province (Lachenbruch and Sass, 1977; Lachenbruch et al., 1994). A persistent mantle upwelling may help to explain the spatial-temporal evolution of volcanism and extension in the Great Basin since mid-Miocene. Most of the bimodal and basaltic volcanism occurred near the margins of the main silicic volcanic field in central Great Basin. In the past 15 Ma or so, volcanism has generally migrated toward the margins of the Great Basin, in concert with block faulting (Armstrong and Ward, 1991) (Fig. 2c). The older (>5 Ma) basaltic rocks typically have isotopic signatures indicating an origin in the mantle lithosphere, whereas the younger basalts occurred mainly near the margins of the Great Basin, have isotopic and elemental compositions indicating an origin of the asthenosphere (Daley and DePaolo, 1992; Harry et al., 1995). Wernicke (1992) suggested that the older basalts also formed by melting of asthenospheric mantle followed by contamination from the mafic lower crust. We have shown in Fig. 13 that the lithospheric mantle surrounding the upwelling asthenosphere may be pushed away and downward in the form of ductile

flow. Most thinning of the lithosphere occurs near the margins of the upwelling asthenosphere where the lateral pressure gradient is the greatest. If the older (>5 Ma) basalts were derived from mantle lithosphere (Leeman and Harry, 1993), then the initial asthenospheric upwelling was below 50–60-km depth. Most mafic melts had to derive from a metasomatized mantle lithosphere (Harry and Leeman, 1995) or a mantle plume (Parsons et al., 1994; Saltus and Thompson, 1995). Melt production waned under central Great Basin, probably when the mantle lithosphere became infertile, and younger volcanism shifted to the margins of the Great Basin where the asthenosphere ascended above 50–60-km depth and melted by decompression. The predicted outward migration of the loci of maximum lithospheric thinning during basin-and-range extension (Fig. 13c) is consistent with the temporal–spatial development of

volcanism and extension in the Great Basin since mid-Miocene. The ductile flow within the lithosphere induced by asthenospheric upwelling predicts a lithospheric structure with the thinnest lithosphere near the margins of the Basin and Range (Fig. 13c). This lithospheric structure is comparable to those observed under the transition zones between the Great Basin and the Sierra Nevada (Fliedner et al., 1996; Wernicke et al., 1996) and the Colorado plateau (Zandt et al., 1995). Liu and Shen (1998b) suggested that this ductile shearing of mantle lithosphere beneath the Basin and Range province may have contributed to the late Cenozoic uplift of the Sierra Nevada mountain ranges (Fig. 16).

4. Discussion

Gravitational collapse has gained wide acceptance in recent years as a viable explanation for both synorogenic and postorogenic extension (Dalmayer and Molnar, 1981; Dewey, 1988; England and Houseman, 1989; Jones et al., 1996; Molnar and Chen, 1983). In this study, we have explored both the potential effects and the limitations of gravitational collapse in the development of Cenozoic extension and volcanism in the North American Cordillera. The complicated tectonic history in this region is difficult, if not impossible, to be fully simulated in a single geodynamic model. Thus, we have chosen to use a combination of simple thermal–rheological and thermomechanical models to explore the dynamic links among core-complex formation, mid-Tertiary volcanism, and basin-and-range extension in Cordillera.

A number of important aspects of gravitational collapse in the Cordillera have not been fully explored in this study. One of them is the relationship between synorogenic extension and postorogenic extension. Cenozoic extension in the North American Cordillera is often compared to active extension in the Tibetan plateau and the High Andes as a later stage of gravitational collapse of orogens (Dalmayer and Molnar, 1981; Dilek and Moores, 1999; Molnar and Chen, 1983). There is some geological evidence for synorogenic extension in the Cordillera dating back to Cretaceous (Applegate and Hodges, 1995; Hodges and Walker, 1992; Wells, 1997). However, it remains unclear if there is any direct link between the synoro-

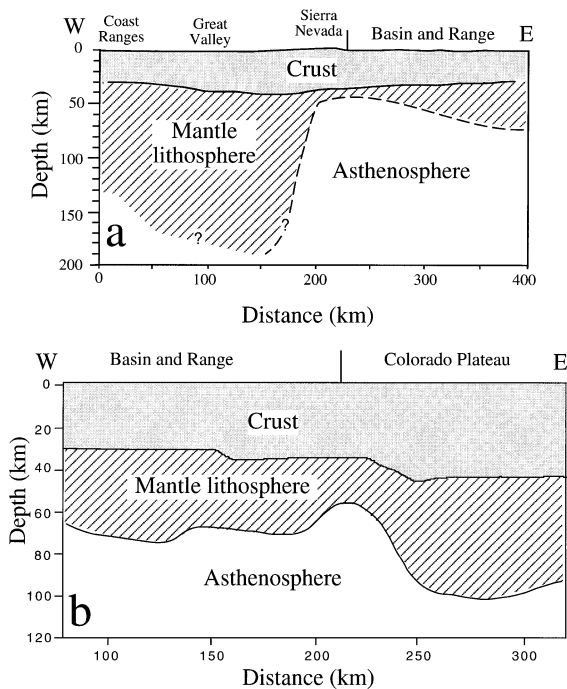


Fig. 16. (a) Lithospheric structure of the Sierra Nevada and surrounding regions from recent geophysical data (Fliedner et al., 1996; Wernicke et al., 1996). (b) Lithospheric structure across the Basin and Range–Colorado Plateau boundary at 37°N latitude. Modified from Zandt et al. (1995). Both (a) and (b) show maximum thinning of the mantle lithosphere near the margin of the Basin and Range province, consistent with model predictions in Fig. 13c.

genic extension and postorogenic extension in the Cordillera, considering that major Cenozoic extension occurred tens of million years after the end of the Cordilleran orogeny (Wernicke et al., 1987). Consequently, further testing is needed for the notion that active extension in the Tibetan plateau and the High Andes may eventually lead to major whole-lithosphere extension as that in the North American Cordillera (Molnar and Chen, 1983). The critical question here is whether or not gravitational collapse of thickened orogenic crust can induce significant mantle upwelling. In models that predict crustal collapse leading to significant whole-lithosphere extension and mantle upwelling, the effects of gravitational collapse were obscured by the imposed lateral stretching in the models (e.g., Govers and Wortel, 1993; Harry et al., 1993). Conversely, other studies have treated the ductile spreading under thickened crust as plane channel flows, assuming complete mechanical decoupling between the crust and mantle. These models predict ductile spreading within the crust that flatten the thickened crust welts into “pancakes” but with little impacts on the mantle lithosphere (Bird, 1991; Hopper and Buck, 1996). Using a flow model with fully coupling between the crust and the mantle, we have shown that gravitational collapse of thickened crust alone cannot induce major asthenospheric mantle upwelling (see Figs. 9 and 10).

The important role of asthenospheric mantle upwelling is not limited to postorogenic extension; England and Houseman (1989) suggested that mantle upwelling under the northern Tibetan plateau was a major drive for active extension in the plateau. To fully understand the geodynamics of gravitational collapse, future studies need to improve our understanding of the causes of asthenospheric mantle upwelling under orogens. For the North American Cordillera, the possible causes include (1) asthenospheric flow following a sagging Farallon plate (Lipman, 1980), (2) the slab window produced by the migrating Mendocino triple junction (Dickinson and Snyder, 1979), (3) a mantle plume (Parsons et al., 1994; Saltus and Lachenbruch, 1991), and (4) removal of thickened mantle lithospheric material by delamination (Bird, 1979) or convective downwelling (Houseman et al., 1981; Houseman and Molnar, 1997). Only the last one was directly related to

the gravitational instability of a thickened lithosphere.

Finally, we need a better understanding of the effects of three-dimensional tectonic boundary conditions on gravitational collapse, some of those were explored by Liu et al. (2000). Given the relatively uniform crustal contraction during the Cordilleran orogeny (Elison, 1991), the large variations of Cenozoic extension and volcanism along the North American Cordillera clearly indicate the influence of tectonic boundary conditions. The occurrence of metamorphic core complexes along the entire Cordilleran orogen may reflect an internal control—the gravitational instability of thickened orogenic crust. However, the development of basin-and-range extension was clearly affected by the evolving plate boundary along the western edge of North America, where the convergent boundary between the Farallon and the North America plates was gradually replaced by the transform boundary along the San Andreas fault system in the past ~ 29 Ma (Atwater, 1970). This change of plate boundaries may have caused not only relaxation of compressional stresses but probably also strongly perturbed the thermal structures of the mantle under the Basin and Range province (Dickinson and Snyder, 1979; Severinghaus and Atwater, 1990). Difference in mantle thermal perturbations, in addition to plate boundary conditions, is also needed to explain the different history of extension and volcanism in the northern and southern Basin and Range provinces. In contrast to the relatively high average elevation, high heat flow, and active extension in the northern Basin and Range province, the southern Basin and Range province has relatively low average elevation, low heat flow, and limited extension that largely ceased in the past 10 Ma (Dokka and Ross, 1995; Glazner and Bartley, 1984; Sonder and Jones, 1999). Inclusion of these tectonic boundary conditions in future geodynamic models will provide a better understanding of the role of gravitational collapse in the Cordillera.

5. Conclusions

(1) Gravitational collapse may have played an important role in Cenozoic extension and magmatism in the North American Cordillera, but both plate boundary processes and mantle thermal perturbations

are needed to fully explain the temporal–spatial evolution of extension and magmatism in this region.

(2) The early phase (>17 Ma) extension including formation of most metamorphic core complexes and the associated plutonism resulted largely from crustal shortening and thickening during the Cordilleran orogeny. Crustal thickening provided excess gravitational potential energy to drive extension, while thermal effects associated with crustal shortening and thickening, including thermal relaxation, enhanced radiogenic heating, shear heating, and possibly localized mantle thermal perturbations, may have caused significant partial melting in the middle to lower crust. High crustal temperature and partial melting allowed gravitational collapse to be largely accommodated by ductile spreading within the lower crust. The diachronous formation of metamorphic core complexes in the Cordillera and their apparent correlation with the abundance of plutonism may reflect the inherited variations in thermal–magmatic history and localized mantle thermal perturbations.

(3) The large-volume silicic volcanism during the mid-Tertiary requires major asthenospheric mantle upwelling to provide heat source for extensive crustal anatexis and parental magma for some of the silicic tuff. This mantle upwelling cannot be directly induced by gravitational collapse of the thickened crust in the Cordilleran orogen. The cause of the mantle upwelling remains speculative. The apparent lack of spatial–temporal correlation between mid-Tertiary volcanism and extension may be explained by the competing effects of thermal weakening and rheological hardening associated with mafic intrusion and underplating.

(4) Basin-and-range extension and the associated bimodal and basaltic volcanism resulted mainly from a persistent mantle upwelling under the Basin and Range province that may be traced back to mid-Tertiary when voluminous volcanic material erupted. Heat advected by the upwelling mantle provided the excess gravitational potential energy for extension, and the lateral pressure gradient induced by the upwelling asthenosphere may have caused significant ductile deformation within the surrounding lithosphere. This asthenosphere–lithosphere interaction can explain the late Cenozoic migration of volcanism and extension toward the margins of the Great Basin and the change of basaltic magma sources from mantle lithosphere to the asthenosphere. The resultant

lithospheric structure, with maximum lithospheric thinning near the margins of the Basin and Range province, is consistent with geophysical observations.

Acknowledgements

Some of the results are based on previous collaborative work with Y. Shen. Youqing Yang did the calculations for Figs. 4 and 12. Constructive review by George Bergantz, Jean-Claude Mareschal, J.L. Vigneresse, and Olivier Vanderhaeghe improved the manuscript. I thank Olivier Vanderhaeghe, Christian Teyssier and Mike Edwards for their efforts in organizing the special GSA symposium on partial melting–postorogenic extension and this spatial Tectonophysics issue. This work was supported by the NSF grants EAR-9506460 and EAR-9805127. Partial support was also provided by the Research Board of the University of Missouri System.

References

- Applegate, J.D.R., Hodges, K.V., 1995. Mesozoic and Cenozoic extension recorded by metamorphic rocks in the Funeral Mountains, California. *Geol. Soc. Am. Bull.* 107, 1063–1076.
- Armijo, R., Tapponnier, P., Mercier, J.L., Han, T.L., 1986. Quaternary extension in Southern Tibet: field observations and tectonic implications. *J. Geophys. Res.* 91, 13803–13872.
- Armstrong, R.L., 1982. Cordilleran metamorphic core complexes— from Arizona to southern Canada. *Annu. Rev. Earth Planet. Sci.* 10, 129–154.
- Armstrong, R.L., Ward, P., 1991. Evolving geographic patterns of Cenozoic magmatism in the North American Cordillera: the temporal and spatial association of magmatism and metamorphic core complexes. *J. Geophys. Res.* 96, 13201–13224.
- Artyushkov, E.V., 1973. Stresses in the lithosphere caused by crustal thickness inhomogeneities. *J. Geophys. Res.* 78, 7675–7690.
- Atwater, T., 1970. Implications of plate tectonics for the Cenozoic tectonic evolution of western North America. *Geol. Soc. Am. Bull.* 81, 3513–3536.
- Axen, G.J., Taylor, W., Bartley, J.M., 1993. Space-time patterns and tectonic controls of Tertiary extension and magmatism in the Great Basin of the western United States. *Geol. Soc. Am. Bull.* 105, 56–72.
- Bennette, R.A., Wernicke, B.P., Davis, J.L., 1998. Continuous GPS measurements of contemporary deformation across the northern Basin and Range province. *Geophys. Res. Lett.* 25, 563–566.
- Best, M.G., Christiansen, E.H., 1991. Limited extension during peak Tertiary volcanism, Great Basin of Nevada and Utah. *J. Geophys. Res.* 96, 13509–13528.

- Bird, P., 1979. Continental delamination and the Colorado Plateau. *J. Geophys. Res.* 84, 7561–7571.
- Bird, P., 1991. Lateral extension of lower crust from under high topography in the isostatic limit. *J. Geophys. Res.* 96, 10275–10286.
- Block, L., Royden, L.H., 1990. Core complex geometries and regional scale flow in the lower crust. *Tectonics* 9, 557–567.
- Bott, M.H.P., 1993. Modeling the plate-driven mechanism. *J. Geol. Soc.* 150, 941–951.
- Bott, M.H.P., Dean, D.S., 1972. Stress systems at young continental margins. *Nature* 235, 23–25.
- Brace, W.F., Kohlstedt, D.L., 1980. Limits on lithospheric stress imposed by laboratory experiments. *J. Geophys. Res.* 85, 6248–6252.
- Burchfiel, B.C., Cowan, D.S., Davis, G.A., 1992. Tectonic overview of the Cordilleran orogen in western United States. In: Burchfiel, B.C., Zoback, M.L., Lipman, P.W. (Eds.), *The Cordilleran Orogen: Conterminous*. U.S. Geol. Soc. Am., Boulder, CO, pp. 407–480.
- Byerlee, J.D., 1978. Friction of rocks. *Pure Appl. Geophys.* 116, 615–626.
- Carslaw, H.S., Jaeger, J.C., 1959. *Conduction of Heat in Solids*. Clarendon Press, Oxford.
- Coney, P.J., 1980. Cordilleran metamorphic core complexes: an overview. *Mem. Geol. Soc. Am.* 153, 7–31.
- Coney, P.J., 1987. The regional tectonic setting and possible causes of Cenozoic extension in the North American Cordillera. In: Coward, M.P., Dewey, J.F., Hancock, P.L. (Eds.), *Continental Extensional Tectonics*. Geol. Soc. (London) Spec. Pub., Oxford, pp. 177–186.
- Coney, P.J., Harms, T.A., 1984. Cordilleran metamorphic core complexes: Cenozoic extensional relics of Mesozoic compression. *Geology* 12, 550–554.
- Coward, M.P., Dewey, J.F., Hancock, P.L. (Eds.), 1987. *Continental Extensional Tectonics*. Geol. Soc. Special Pub., vol. 28. Blackwell, Oxford, 637 pp.
- Daley, E.E., DePaolo, D.J., 1992. Isotopic evidence for lithospheric thinning during extension: southeastern Great Basin. *Geology* 20, 104–108.
- Dalmayer, B., Molnar, P., 1981. Parallel thrust and normal faulting in Peru and constrains on the state of stress. *Earth Planet. Sci. Lett.* 55, 473–481.
- Dewey, J.F., 1988. Extensional collapse of orogens. *Tectonics* 7, 1123–1139.
- Dickinson, W.R., Snyder, W.S., 1979. Geometry of subducted slabs related to the San Andreas transform. *J. Geol.* 87, 609–627.
- Dilek, Y., Moores, E., 1999. A Tibetan model for the early Tertiary western United States. *J. Geol. Soc. (London)* 156, 929–941.
- Dixon, T.H., Robaudo, S., Lee, J., Reheis, M.C., 1995. Constraints on present-day Basin and Range deformation from space geodesy. *Tectonics* 14, 755–772.
- Dokka, R.K., Ross, T.M., 1995. Collapse of southwestern North America and the evolution of early Miocene detachment faults, metamorphic core complexes, the Sierra Nevada orocline, and the San Andreas fault system. *Geology* 23, 1075–1078.
- Eaton, G.P., 1982. The Basin and Range Province: origin and tectonic significance. *Annu. Rev. Earth Planet. Sci.* 10, 409–440.
- Eaton, G.P., Wahl, R.R., Prostka, H.J., Mahey, D.R., Kleinkopf, M.D., 1978. Regional gravity and tectonic patterns: their relation to late Cenozoic epeirogeny and lateral spreading in the western Cordillera. In: Smith, R.B., Eaton, G.P. (Eds.), *Cenozoic Tectonics and Regional Geophysics of the Western Cordillera*. Geol. Soc. Am. Mem., Boulder, CO, pp. 51–91.
- Elison, M.W., 1991. Intracontinental contraction in western North America: continuity and episodicity. *Geol. Soc. Am. Bull.* 103, 1226–1238.
- England, P., 1993. Convective removal of thermal boundary layer of thickened continental lithosphere: a brief summary of causes and consequences with special reference to the Cenozoic tectonics of the Tibetan Plateau and surrounding regions. *Tectonophysics* 223, 67–73.
- England, P.C., Houseman, G.A., 1989. Extension during continental convergence with special reference to the Tibetan plateau. *J. Geophys. Res.* 94, 17561–17597.
- England, P.C., McKenzie, D.P., 1982. A thin viscous sheet model for continental deformation. *J. Geophys. Res.* 70, 295–321.
- England, P.C., Molnar, P., 1993. The interpretation of inverted metamorphic isogrades using simple physical calculations. *Tectonics* 12, 145–157.
- England, P.C., Richardson, S.W., 1977. The influence of erosion upon the mineral facies of rocks from different metamorphic environments. *J. Geol. Soc. (London)* 134, 201–213.
- England, P.C., Thompson, A.B., 1984. Pressure–temperature–time paths of regional metamorphism I: heat transfer during the evolution of regions of thickened continental crust. *J. Petrol.* 25, 894–928.
- England, P., Le Fort, P., Molnar, P., Pecher, A., 1992. Heat sources for Tertiary metamorphism and anatexis in the Annapurna–Manaslu region center Nepal. *J. Geophys. Res.* 97, 2107–2128.
- Fleitout, L., Froidevaux, C., 1982. Tectonics and topography for a lithosphere containing density heterogeneities. *Tectonics* 1, 21–56.
- Flidner, M.M., Ruppert, S., The Southern Sierra Nevada Continental Dynamics Working Group, 1996. Three-dimensional crustal structure of the southern Sierra Nevada from seismic fan profiles and gravity modeling. *Geology* 24, 367–370.
- Forsyth, D., Uyeda, S., 1975. On the relative importance of the driving forces of plate motion. *Geophys. J. R. Astron. Soc.* 43, 163–200.
- Gans, P.B., Mahood, G.A., Schermer, E., 1989. Synextensional magmatism in the Basin and Range Province: a case study from the eastern Great Basin. *Geol. Soc. Am., Spec. Pap.* 233, 1–58, Boulder, CO.
- Glazner, A.F., Bartley, J.M., 1984. Timing and tectonic setting of Tertiary low-angle normal faulting and associated magmatism in the southwestern United States. *Tectonics* 3, 385–396.
- Glazner, A.F., Bartley, J.M., 1985. Evolution of lithospheric strength after thrusting. *Geology* 13, 42–45.
- Govers, R., Wortel, M.J.R., 1993. Initiation of asymmetric extension in continental lithosphere. *Tectonophysics* 223, 75–96.
- Grunder, A.L., 1995. Material and thermal roles of basalt in crustal magmatism: case study from eastern Nevada. *Geology* 23, 952–956.
- Harrison, T.M., Lovera, O.M., Grove, M., 1997. New insights into

- the origin of two contrasting Himalayan granite belts. *Geology* 25, 899–902.
- Harrison, T.M., Grove, M., Lovera, O.M., Catlos, E.J., 1998. A model for the origin of Himalayan anatexis and inverted metamorphism. *J. Geophys. Res.* 103, 27017–27032.
- Harry, D.L., Leeman, W.P., 1995. Partial melting of melt metasomatized subcontinental mantle and the magma source potential of the lower lithosphere. *J. Geophys. Res.* 100, 10255–10270.
- Harry, D.L., Sawyer, D.S., Leeman, W.P., 1993. The mechanics of continental extension in western North America: implications for the magmatic and structural evolution of the Great Basin. *Earth Planet. Sci. Lett.* 117, 59–71.
- Harry, D.L., Oldow, J.S., Sawyer, D.S., 1995. The growth of orogenic belts and the role of crustal heterogeneities in decollement tectonics. *Geol. Soc. Am. Bull.* 107, 1411–1426.
- Hawkesworth, C., et al., 1995. Calc-alkaline magmatism, lithospheric thinning and extension in the Basin and Range. *J. Geophys. Res.* 100, 10271–10286.
- Hildreth, W., 1981. Gradients in silicic magma chambers: implications for lithospheric magmatism. *J. Geophys. Res.* 86, 10153–10192.
- Hodges, K.V., Walker, J.D., 1992. Extension in the Cretaceous Sevier orogen, North American Cordillera. *Geol. Soc. Am. Bull.* 104, 560–590.
- Hooper, P.R., Bailey, D.G., Holder, G.A.M., 1995. Tertiary calc-alkaline magmatism associated with lithospheric extension in the Pacific Northwest. *J. Geophys. Res.* 100, 10303–10320.
- Hopper, J.R., Buck, W.R., 1996. The effects of lower crust flow on continental extension and passive margin formation. *J. Geophys. Res.* 101, 20175–20194.
- Houseman, G.A., Molnar, P., 1997. Gravitational (Rayleigh–Taylor) instability of a layer with non-linear viscosity and convective thinning of continental lithosphere. *Geophys. J. Int.* 128, 125–150.
- Houseman, G.A., McKenzie, D.P., Molnar, P., 1981. Convective instability of a thickened boundary layer and its relevance for the thermal evolution of continental convergent belts. *J. Geophys. Res.* 86, 6115–6132.
- Huerta, A.D., Royden, L.H., Hodges, K.V., 1998. The thermal structure of collisional orogens as a response to accretion, erosion, and radiogenic heat production. *J. Geophys. Res.* 103, 15287–15302.
- Jamieson, R.A., Beaumont, C., Fullsack, P., Lee, B., 1998. Barrovian regional metamorphism: where's the heat. In: Treloar, P.J., O'Brien, P.J. (Eds.), *What Drives Metamorphism and Metamorphic Reactions?* *Geol. Soc. (London) Spec. Pub.*, Oxford, pp. 23–51.
- Johnson, C.M., 1991. Large-scale crustal formation and lithosphere modification beneath Middle to Late Cenozoic calderas and volcanic fields, western North America. *J. Geophys. Res.* 96, 13485–13508.
- Jones, C.H., Unruh, J.R., Sonder, L.J., 1996. The role of gravitational potential energy in active deformation in the southwestern United States. *Nature* 381, 37–41.
- Karato, S.I., Paterson, M.S., Fitzgerald, J.D., 1986. Rheology of synthetic olivine aggregates: influence of grain-size and water. *J. Geophys. Res.* 91, 8151–8176.
- Kirby, S.H., Kronenberg, A.K., 1987. Rheology of the lithosphere: selected topics. *Rev. Geophys.* 25, 1219–1244.
- Kruse, S., McNutt, M., Phipps-Morgan, J., Royden, L., Wernicke, B., 1991. Lithospheric extension near Lake Mead, Nevada: a model for ductile flow in the lower crust. *J. Geophys. Res.* 96, 4435–4456.
- Kusznir, N.J., Park, R.G., 1984. Intraplate lithosphere deformation and the strength of the lithosphere. *Geophys. J. R. Astron. Soc.* 79, 513–538.
- Lachenbruch, A.H., 1970. Crustal temperature and heat production: implications of the linear heat flow relation. *J. Geophys. Res.* 75, 3291–3300.
- Lachenbruch, A., Sass, J., 1977. Heat flow in the United States and the thermal regime of the crust. *The Earth's Crust: Its Nature and Physical Properties*. *Geophys. Monogr. Ser.*, vol. 20. Am. Geophys. Union, Washington, pp. 626.
- Lachenbruch, A.H., Sass, J.H., 1978. Models of an extending lithosphere and heat flow in the Basin and Range Province. In: Smith, R.B., Eaton, G.P. (Eds.), *Cenozoic Tectonics and Regional Geophysics of the Western Cordillera*. *Geol. Soc. Am. Mem.*, Boulder, CO, pp. 209–250.
- Lachenbruch, A.H., Sass, J.H., Morgan, P., 1994. Thermal regime of the southern Basin and Range Province, 2, Implications of heat flow for regional extension and metamorphic core complexes. *J. Geophys. Res.* 99, 22121–22136.
- Leeman, W.P., Harry, D.L., 1993. A binary source model for extension-related magmatism in the Great Basin, western North America. *Science* 262, 1550–1554.
- Le Pichon, X., 1982. Land-locked oceanic basins and continental collision. In: Hui, K. (Ed.), *Mountain Building Processes*. Academic Press, London, pp. 210–212.
- Lipman, P.W., 1980. Cenozoic volcanism in the western United States: implication for continental tectonics. *Studies in Geophysics: Continental Tectonics*. National Academy of Sciences, Washington, DC, pp. 161–174.
- Lipman, P.W., Glazner, A.F., 1991. Introduction to middle Tertiary Cordilleran volcanism: magma sources and relations to regional tectonics. *J. Geophys. Res.* 96, 13193–13199.
- Lipman, P.W., Prostka, H.J., Christiansen, R.L., 1971. Evolving subduction zones in the western United States, as interpreted from igneous rocks. *Science* 174, 821–825.
- Lipman, P.W., Prostka, W.J., Christiansen, R.L., 1972. Cenozoic volcanism and plate tectonic evolution of the western United States; Part I, Early and Middle Cenozoic. *R. Soc. London Philos. Trans.* 271-A, 217–248.
- Lister, G.S., Baldwin, S.L., 1993. Plutonism and the origin of metamorphic core complexes. *Geology* 21, 607–614.
- Liu, M., 1996. Dynamic interactions between crustal shortening, extension, and magmatism in the North American Cordillera. *Pure Appl. Geophys.* 146, 447–467.
- Liu, M., Chase, C.G., 1991. Evolution of Hawaiian basalts: a hot-spot melting model. *Earth Planet. Sci. Lett.* 104, 151–165.
- Liu, M., Furlong, K.P., 1993. Crustal shortening and Eocene extension in the southeastern Canadian Cordillera: some thermal and mechanical considerations. *Tectonics* 12, 776–786.
- Liu, M., Furlong, K.P., 1994. Intrusion and underplating of mafic magmas: thermal–rheological effects and implications for Ter-

- tiary tectonomagmatism in the North American Cordillera. *Tectonophysics* 273, 175–187.
- Liu, M., Shen, Y., 1998a. Crustal collapse, mantle upwelling, and Cenozoic extension of the North American Cordillera. *Tectonics* 171, 311–321.
- Liu, M., Shen, Y., 1998b. The Sierra Nevada uplift: a ductile link to mantle upwelling under the Basin and Range. *Geology* 26, 299–302.
- Liu, M., Shen, Y., Yang, Y., 2000. Gravitational collapse of orogenic crust: a preliminary 3D finite element study. *J. Geophys. Res.* 105, 3159–3173.
- Livaccari, R.F., 1991. Role of crustal thickening and extensional collapse in the tectonic evolution of the Sevier–Laramide orogeny, western United States. *Geology* 19, 1104–1107.
- Lynch, H.D., Morgan, P., 1987. The tensile strength of the lithosphere and the localization of extension. In: Coward, M.P., Dewey, J.F., Hancock, P.L. (Eds.), *Continental Extensional Tectonics*. Geol. Soc. (London) Spec. Pub., Oxford, pp. 53–66.
- Mayer, L. (Ed.), 1986. *Extensional Tectonics of the Southwestern United States: A Perspective on Progresses and Kinematics*, Special Paper 208. Geol. Soc. Am., Boulder, CO, pp. 10–122.
- McCarthy, J., Larkin, S.P., Futs, G.S., Simpson, R.W., Howard, K.A., 1991. Anatomy of a metamorphic core complex: seismic refraction/wide-angle reflection profiling in southeastern California and western Arizona. *J. Geophys. Res.* 96, 12259–12291.
- McKenzie, D., Bickle, M.J., 1988. The volume and composition of melt generated by extension of the lithosphere. *J. Petrol.* 29, 625–679.
- Mercier, J.L., 1981. Extensional–compressional tectonics associated with the Aegean arc: comparison with the Andean cordillera of south Peru–north Bolivia. *Philos. Trans. R. Soc. London* 300, 337–355.
- Mercier, J.L., et al., 1992. Changes in the tectonic regime above a subduction zone of Andean type: the Andes of Peru and Bolivia during the Pliocene–Pleistocene. *J. Geophys. Res.* 97, 11945–11982.
- Metcalfe, R.V., Smith, E.I., 1995. Introduction to special section: magmatism and extension. *J. Geophys. Res.* 100 (B6), 10249–10254.
- Molnar, P., Chen, W.-P., 1983. Focal depths and fault plane solutions of earthquakes under the Tibetan plateau. *J. Geophys. Res.* 88, 1180–1196.
- Molnar, P., England, P., 1990. Temperatures, heat flux, and frictional stress near major thrust faults. *J. Geophys. Res.* 95, 4833–4856.
- Molnar, P., Lyon-Caen, H., 1988. Some simple physical aspects of the support, structure, and evolution of mountain belts. *Geol. Soc. Am., Spec. Pap.* 218, 179–207.
- Nabelek, P., Liu, M., 1999a. Thermo-rheological shear-heating model for leucogranite generation during crustal convergence. *EOS Trans. AGU* 80 (17), S345 (Abstract).
- Nabelek, P.I., Liu, M., 1999b. Petrogenesis of leucogranites in the Balk Hills, South Dakota, as the consequence of shear heating during thrusting. *Geology* 27, 523–526.
- Oxburgh, E.R., Turcotte, D.L., 1974. Membrane tectonics and the East African Rift. *Earth Planet. Sci. Lett.* 22, 133–140.
- Parrish, R.R., Carr, S.D., Parkinson, D.L., 1988. Eocene extensional tectonics and geochronology of the southern Omineca belt, British Columbia and Washington. *Tectonics* 7, 181–212.
- Parsons, B., McKenzie, D.P., 1978. Mantle convection and the thermal structure of the plates. *J. Geophys. Res.* 83, 4495–4496.
- Parsons, T., Thompson, G.A., Sleep, N., 1994. Mantle plume influence on the Neogene uplift and extension of the U.S. western Cordillera? *Geology* 22, 83–86.
- Peacock, S.M., 1989. Thermal modeling of metamorphic pressure–temperature–time paths: a forward approach. In: Spear, F.S., Peacock, S.M. (Eds.), *Metamorphic Pressure–Temperature–Time Paths*. Short Courses in Geology American Geophysical Union, Washington, DC, pp. 57–102.
- Ranalli, G., 1995. *Rheology of the Earth*. Chapman & Hall, London, 413 pp.
- Ranalli, G., Murphy, D.C., 1987. Rheological stratification of the lithosphere. *Tectonophysics* 132, 281–295.
- Ranalli, G., Brown, R.L., Bosdachin, R., 1989. A geodynamic model for extension in the Shuswap core complex, southeastern Canadian Cordillera. *Can. J. Earth Sci.* 26, 1647–1653.
- Ruppel, C., Royden, L., Hodges, K.V., 1988. Thermal modeling of extensional tectonics: application to the pressure–temperature–time histories of metamorphic rocks. *Tectonics* 7, 947–957.
- Rutter, E.H., Brodie, K.H., 1988. The role of tectonic grain size reduction in the rheological stratification of the lithosphere. *Geol. Rundsch.* 77, 295–308.
- Saltus, R.W., Lachenbruch, A.H., 1991. Thermal evolution of the Sierra Nevada: tectonic implications of new heat flow data. *Tectonics* 10, 325–344.
- Saltus, R.W., Thompson, G.A., 1995. Why is it downhill from Tonopah to Las Vegas? a case for mantle plume support of the high northern Basin and Range. *Tectonics* 14, 1235–1244.
- Sass, J.H., et al., 1994. Thermal regime of the southern Basin and Range Province, I, Heat flow data from Arizona and the Mojave Desert of California and Nevada. *J. Geophys. Res.* 99, 22093–22120.
- Sengor, A.M.C., Burke, K., 1978. Relative timing of rifting and volcanism on earth and its tectonic implications. *Geophys. Res. Lett.* 5, 419–421.
- Severinghaus, J., Atwater, T., 1990. Cenozoic geometry and thermal state of the subducting slabs beneath western North America. In: Wernicke, B.P. (Ed.), *Basin and Range Extensional Tectonics Near the Latitude of Las Vegas, Nevada*. Geol. Soc. Am. Mem., Boulder, CO, pp. 1–22.
- Shen, Y., 1997. Gravitational collapse of orogenic belts: a preliminary study. PhD Thesis, University of Missouri, Columbia, 273 pp.
- Shi, Y., Wang, C.-Y., 1987. Two-dimensional modeling of the P–T–t paths of regional metamorphism in simple overthrust terrains. *Geology* 15, 1048–1051.
- Shi, Y., Zhu, Y., 1993. Some aspects of thermotectonics of the Tibetan plateau. *Tectonophysics* 219, 223–233.
- Smith, R.B., et al., 1989. Geophysical and tectonic framework of the eastern Basin and Range–Colorado Plateau–Rocky Mountain transition. In: Pakiser, L.C., Mooney, W.D. (Eds.), *Geophysical Framework of the Continental United States*. Geol. Soc. Am. Mem., Boulder, CO, pp. 205–233.

- Smrekar, S.E., Solomon, S.C., 1992. Gravitational spreading of high terrain in Ishtar Terra, Venus. *J. Geophys. Res.* 97, 16121–16148.
- Sonder, L.J., Jones, C.H., 1999. Western United States extension: how the west was widened. *Annu. Rev. Earth Planet. Sci.* 27, 417–462.
- Sonder, L.J., England, P.C., Wernicke, B., Christiansen, R.L., 1987. A physical model for Cenozoic extension of western North America. In: Coward, M.P., Dewey, J.F., Hancock, P.L. (Eds.), *Continental Extensional Tectonics*. Geol. Soc. (London) Spec. Pub., Oxford, pp. 187–201.
- Spencer, J.E., et al., 1995. Spatial and temporal relationships between mid-Tertiary magmatism and extension in southwestern Arizona. *J. Geophys. Res.* 100, 10321–10352.
- Stewart, J.H., 1978. Basin and Range structure in western North America: a review. In: Smith, R.B., Eaton, G.L. (Eds.), *Cenozoic Tectonics and Regional Geophysics of the Western Cordillera*. Mem. Geol. Soc. Am., Boulder, CO, pp. 1–31.
- Taylor, W.J., Bartley, J.M., Lux, D.L., Axen, G.J., 1989. Timing of Tertiary extension in the Railroad Valley–Pioche transect, Nevada: constraints from $^{40}\text{Ar}/^{39}\text{Ar}$ ages of volcanic rocks. *J. Geophys. Res.* 94, 7757–7774.
- Thompson, R.N., 1975. Primary basaltic magma genesis, II, Snake River Plain, Idaho, USA. *Contrib. Mineral. Petrol.* 52, 213–232.
- Vanderhaeghe, O., Teyssier, C., 1997. Formation of the Shuswap metamorphic core complex during late-orogenic collapse of the Canadian Cordillera: role of ductile thinning and partial melting of the mid-to lower crust. *Geodin. Acta (Paris)* 10, 41–58.
- Wells, M.L., 1997. Alternating contraction and extension in the hinterlands of orogenic belts: an example from the Raft River Mountains, Utah. *Geol. Soc. Am. Bull.* 109, 107–126.
- Wenrich, K.J., Billingsley, G.H., Blackerby, B.A., 1995. Spatial migration and compositional changes of Miocene–Quaternary magmatism in the Western Grand Canyon. *J. Geophys. Res.* 100, 10417–10440.
- Wernicke, B.P., 1992. Cenozoic extensional tectonics of the U.S. Cordillera. In: Burchfiel, B.C., Zoback, M.L., Lipman, P.W. (Eds.), *The Cordilleran Orogen: Conterminous*. U.S. Geol. Soc. Am., Boulder, CO, pp. 553–581.
- Wernicke, B., Christiansen, R.L., England, P.C., Sonder, L.J., 1987. Tectonomagmatic evolution of Cenozoic extension in the North American Cordillera. In: Coward, M.P., Dewey, J.F., Hancock, P.L. (Eds.), *Continental Extensional Tectonics*. Geol. Soc. Spec. Pub., Boulder, CO, pp. 203–221.
- Wernicke, B.P., et al., 1996. Origin of high mountains in continents: the southern Sierra Nevada. *Science* 271, 190–193.
- Williams, C.A., Richardson, R.M., 1991. A rheological layered three-dimensional model of the San Andreas Fault in central and southern California. *J. Geophys. Res.* 96, 16597–16623.
- Yuen, D.A., Fleitout, L., Schubert, G., Froidevaux, C., 1978. Shear deformation along major transform faults and subduction slabs. *J. R. Astron. Soc.* 54, 93–120.
- Zandt, G., Myers, S.C., Wallace, T.C., 1995. Crust and mantle structure across the Basin and Range–Colorado Plateau boundary at 37°N latitude and implications for Cenozoic extensional mechanism. *J. Geophys. Res.* 100, 10529–10548.
- Zen, E.-A., 1988. Thermal modeling of stepwise anatexis in a thrust-thickened sialic crust. *Trans. R. Astron. Soc. Edinburgh* 79, 223–235.
- Zoback, M.D., Anderson, R.E., Thompson, G.A., 1981. Cenozoic evolution of the state of stress and style of tectonism of the Basin and Ranges Province of the western United States. *Philos. Trans. R. Soc. London, Ser. A* 300, 407–434.